ΕΛΛΗΝΙΚΗ
ΕΠΙΣΤΗΜΟΝΙΚΗ
ΕΤΑΙΡΕΙΑ
ΕΔΑΦΟΜΗΧΑΝΙΚΗΣ
& ΓΕΩΤΕΧΝΙΚΗΣ
ΜΗΧΑΝΙΚΗΣ

Τα Νέα

της Ε Ε Ε Ε Γ Μ

86

Αρ. 86 – ΙΑΝΟΥΑΡΙΟΣ 2016

Σιδηροδρομική γέφυρα στην Ελβετία

Π Ε Ρ Ι Ε Χ Ο Μ Ε Ν Α

Η θέα από ένα ύψος 8000 μέτρων.

Κρυσταλλωμένα Παγόβουνα.

Δάδα σε σπήλαιο πάγου.

ΑΡΘΡΑ

Παρουσίαση άρθρων, στην συγγραφή των οποίων μετείχαν Έλληνες, στο XVI European Conference on Soil Mechanics and Geotechnical Engineering, Edinburgh, 13-17 September 2015 (κατ' αλφαβητική σειρά, στα ελληνικά, του ονόματος του πρώτου συγγραφέα).

Stiffness anisotropy and its effect on the behaviour of deep excavations

L'anisotropie de déformabilité et ses effets sur les modes de comportement des excavations profondes

A. Grammatikopoulou, F.C. Schroeder, N. Kovacevic and D.M. Potts

ABSTRACT This paper examines the effect of stiffness anisotropy on the behaviour of a deep excavation in a stiff plastic clay, such as London Clay. A cross anisotropic non-linear elasto-plastic model which has previously been validated against advanced laboratory tests is used to simulate the London Clay. The predictions of this anisotropic model are compared with those of an isotropic model which has been used extensively in the past to simulate the behaviour of such clays. Three propping systems are considered, a single-propped wall, a double-propped wall and a multi-propped wall. The study examines the effect of stiffness anisotropy on the patterns of behaviour both in the short and long term.

1 INTRODUCTION

The stiffness of stiff plastic clays is known to be nonlinear as well as anisotropic. The effect of nonlinearity has been the subject of numerous studies and it is now well known that, in order to obtain accurate predictions of movements induced in the ground, it is necessary to account for it. However, the effect of stiffness anisotropy has not been studied in such detail; only a limited number of studies have investigated the effect of stiffness anisotropy on predictions of movements resulting from geotechnical construction activities (e.g. Grammatikopoulou et al. 2011, Jurecic 2012).

This study examines the effect of stiffness anisotropy on the behaviour of a deep excavation in a stiff plastic clay. It is a continuation of the work of Grammatikopoulou et al. (2011) in that it uses the same cross-anisotropic non-linear elasto-plastic model (Franzius et al. 2005) to simulate the behaviour of stiff plastic London Clay. Predictions using this model are compared with the predictions of an isotropic non-linear elasto-plastic model (Jardine et at. 1986, 1991) which has been used extensively in the past to successfully simulate the behaviour of London Clay in a variety of boundary value problems (Hight & Higgins 1995, St. John et al. 1992). The paper examines how accounting for stiffness anisotropy affects the patterns of behaviour both in the short-term and in the long-term. The effect of stiffness anisotropy is examined for three different propping systems: a single-propped wall, a doublepropped wall and a multi-propped wall.

2 PROBLEM ANALYSED

The problem analysed considers an excavation for a three level basement in London. The assumed geometry and soil stratigraphy can be seen in Figure 1.

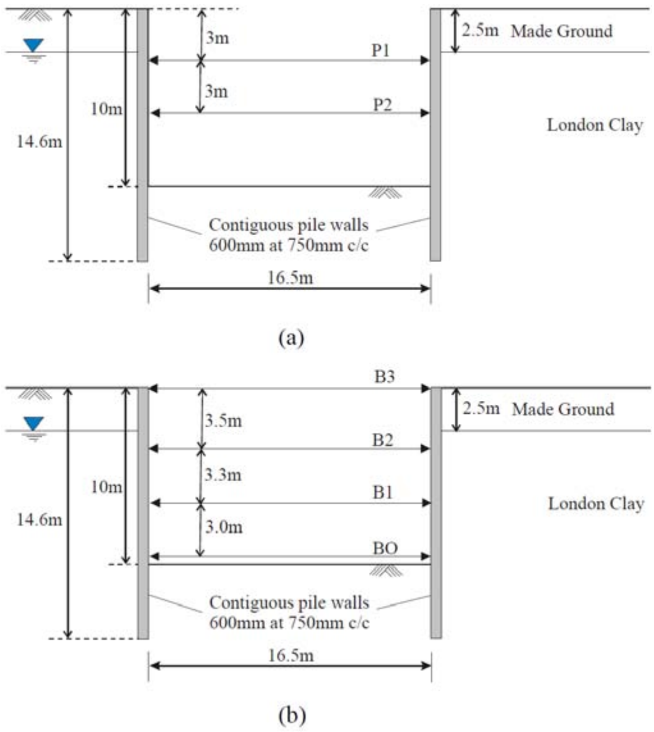

Figure 1. Geometry for a) single and doubled-propped walls b) multi-propped wall constructed using top down construction.

The walls retaining the excavation are assumed to be contiguous bored pile walls with a pile diameter of 600 mm at 750 mm spacing. Three propping systems are considered. In the first case a single prop, P1, is assumed to support the walls during the excavation, whereas in the second case two props, P1 and P2, are assumed (refer to Figure 1a). In the third case a multi-propped excavation constructed using a top-down construction methodology is considered (see Figure 1b). Cases 1 and 2 represent temporary support systems, whereas case 3 is a permanent and temporary support system. In cases 1 and 2 the temporary props are replaced in the permanent condition by the permanent slabs (B0 to B3) shown in Figure 1b.

The soil profile, assumed in the analyses, is typical of the conditions encountered in London. A 2.5 m thick layer of Made Ground is assumed to overlie the London Clay deposit which, in turn, is assumed to extend to a depth of 74 m.

3 CONSTITUTIVE SOIL MODELS

3.1 Anisotropic model

A number of studies have shown that the small strain stiffness of stiff plastic clays can be interpreted within the framework of cross-anisotropic elasticity (Lings et al. 2000, Gasparre et al. 2007). In the light of these research findings, Grammatikopoulou et al. (2011) and Jurecic (2012) used the cross-anisotropic non-linear elasto-plastic model of Franzius et al. (2005) to simulate the behaviour of London Clay.

This model combines a three-parameter crossanisotropic formulation (Graham & Houslby 1983) with a non-linear elastic response. The anisotropy is defined by 3 independent parameters: E'_v, the drained Young's modulus in the vertical direction, ν'_{hh} the drained Poisson's ratio for horizontal strain due to horizontal strain and the anisotropic scale factor α:

$$\alpha = \sqrt{\frac{E'_h}{E'_v}} = \frac{\nu'_{hh}}{\nu'_{vh}} = \frac{G_{hh}}{G_{hv}} \tag{1}$$

where E'_h is the drained horizontal Young's modulus, ν'_{vh} is the drained Poisson's ratio for vertical strains due to horizontal strains, G_{hh} is the shear modulus in the horizontal plane and G_{hv} is the shear modulus in the vertical plane. The non-linearity in the model is achieved by allowing the normalized vertical drained Young's modulus E'_v/p' (where p' is the mean effective stress) to vary with deviatoric strain (Franzius et al. 2005). The plastic part of the model is provided by a Mohr-Coulomb yield surface and a non-associated flow rule.

Grammatikopoulou et al. (2011) presented simulations of laboratory tests from the advanced investigation of London Clay from London's Heathrow Airport Terminal 5 (T5) (Gasparre et al. 2007, Hight et al. 2007) and showed how this model can reproduce well the response measured in these advanced tests.

On this basis, the same anisotropic model was also employed in this study in order to model the behavior of London Clay. For further details on the equations of the model the reader is referred to the original publications (Franzius et al. 2005). For information on the derivation of the model parameters for London Clay the reader is referred to Grammatikopoulou et al. (2011).

3.2 Isotropic model

The isotropic model adopted for the simulation of the London Clay is a non-linear model of the form outlined by Jardine et al. (1986). In this isotropic model the normalised shear modulus, G/p', is allowed to vary with deviatoric strain and the normalized bulk modulus K/p' is allowed to vary with volumetric strain. The equations describing the variations of G and K can be found in Franzius et al. (2005). As for the anisotropic model, the plastic part of the model is provided by a Mohr-Coulomb yield surface and a non-associated flow rule.

Grammatikopoulou et al (2011) also employed the same isotropic model in their study. The parameters of the isotropic model were chosen such that both isotropic and anisotropic models matched the stiffness response measured in the undrained triaxial tests from the T5 research. Figure 2 shows the model simulations for an undrained triaxial compression test from this research (A3 38.7m). However, the effective stress paths and pore water pressures generated by each model are different. Moreover, simulations of oedometer tests show a generally softer response for the anisotropic model.

4 FINITE ELEMENT ANALYSES

4.1 Analyses details

For each propping system two analyses were carried out; one in which the London Clay was modeled with the anisotropic model and one in which it was modelled with the isotropic model. In both sets of analyses the Made Ground was modelled as a linear elastic perfectly plastic material with a Mohr-Coulomb yield surface and a non-associated flow rule. The model parameters for both London Clay and Made Ground were taken from Grammatikopoulou et al. (2011).

The retaining walls were modelled using solid elements with a thickness of 600mm. In order to take account of the out of plane spacing of the piles the Young's modulus was adjusted such that the wall's bending stiffness was replicated. Full friction was assumed at the interface between the walls and the soil. The walls were "wished in place", i.e. their installation was not modelled.

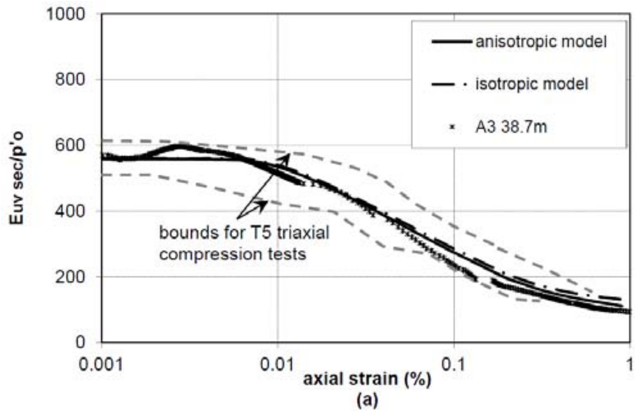

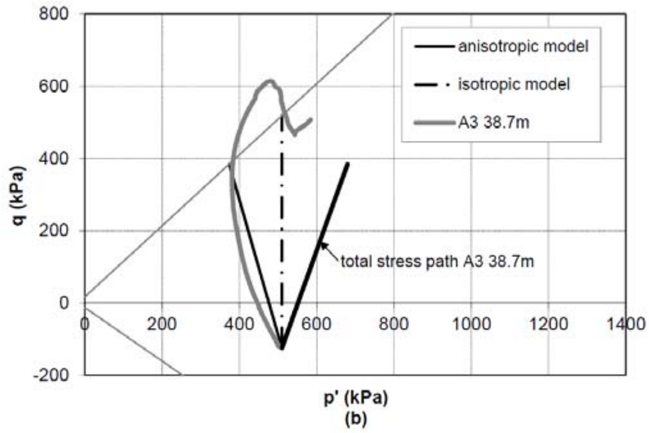

Figure 2. Comparison of model predictions and experimental data for an undrained triaxial compression test from T5 a) secant normalized E_{uv} against axial strain b) stress path.

The temporary props, P1 and P2, and the permament slabs, B0, B1, B2 and B3 were modeled as springs. In cases 1 and 2, P1 and P2 were installed once the excavation reached a level of 0.5 m below each prop level. Once the formation level was reached, B0, B1, B2 and B3 were installed and the corresponding temporary props were removed. The building loads were then applied as a uniformly distributed load equal to 50kPa at formation level.

In case 3, B3 was installed before any excavation took place. B2 and B1 were then constructed once the excavation level reached 1 m and 0.5 m below each slab level respectively. B0 was constructed once the excavation reached the final level.

A stiffness equal to 75 MN/m/m was assigned to P1 and P2. B1, B2 and B3 were assigned a stiffness equal to 200 MN/m/m while B0 had a stiffness of 150 MN/m/m. This was based on slab thicknesses of 325 mm and 250 mm respectively and a Young's modulus equal to 10MPa (chosen to account for openings in the slabs).

A hydrostatic pore water pressure profile with a water table at a depth of 2.5m was assumed. The K_0 distribution was as assumed by Grammatikopoulou et al. (2011); 0.5 in the Made Ground and 1.5 at the top of the London Clay gradually reducing with depth.

The analyses were fully coupled. The Made Ground was modelled as drained material. For the London Clay the permeability, k, was assumed to be related to the mean effective stress, p', as follows: $k = k_o\, e^{-Dp'}$ with k_o = 1x10-9 m/s and D = 0.007. During excavation and load application very small time steps were used which, combined with the low permeability of the strata, resulted in approximately undrained conditions for the London Clay. In the long term the excess pore pressures were allowed to dissipate fully to steady state conditions. A zero pore water pressure boundary condition was applied at formation level in the long term, i.e. it was assumed that any excess water would be pumped.

The analyses were carried out using the finite element code ICFEP. All the analyses were plane strain and used eight node isoparametric quadrilateral elements with 2x2 integration. A modified Newton-Raphson scheme, with an error controlled substepping algorithm, was used as the non-linear solver (Potts & Zdravkovic 1999).

4.2 Analyses results

Figure 3 shows horizontal wall movements for cases 1 to 3 in the short term (after the load application) and in the long term, predicted by the isotropic and anisotropic models. This figure shows that the propping system has a bigger effect than anisotropy. Furthermore, in the short term the anisotropic model predicts smaller movements than the isotropic model, irrespective of the propping system. Similar findings were reported by Jurecic et al. (2012) in the numerical analysis of a deep excavation at Moorgate. In the current study, the maximum horizontal deflection predicted by the anisotropic model is 40mm, 22mm and 16mm for cases 1, 2 and 3 respectively. These values are 9%, 12% and 15% smaller than the maximum deflection predicted by the isotropic model.

Based on observed deflections of retaining walls in London Clay, Gaba et al (2003) suggest that high support systems (i.e. top down construction) are expected to have maximum deflections less than 0.2%H (where H is the maximum excavation depth) and typically in the order of 0.15%H. For the 10m deep excavation analysed, 0.15%H is 15mm which compares well with the predictions of the anisotropic model for case 3. Typical values for cantilever walls are in the order of 0.4%H, i.e. 40mm for H=10m. Case 1, with a low support stiffness system, would be expected to result in smaller deflections than the cantilever wall. The maximum predicted deflection of the anisotropic model for case 1 compares better with this latter value than the isotropic model, although it seems to be on the high side of the measurements.

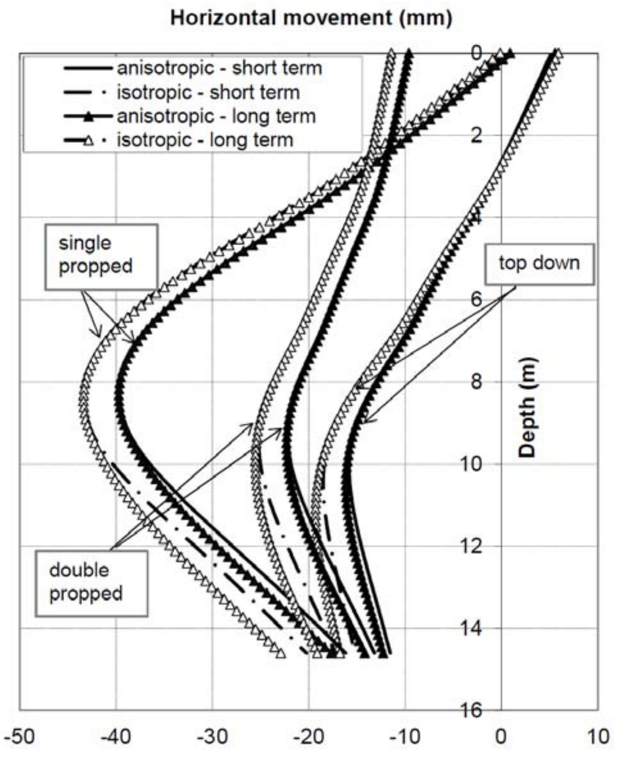

Figure 3. Horizontal wall movements in the short and long term

In the long term the maximum horizontal wall deflections remain practically the same with only a small increase in the movement at the toe. This indicates a stiff permanent support system for all cases.

Figure 4 shows the surface settlement profiles behind the wall for cases 1 and 3. In case 1 the isotropic model predicts higher settlement, than the anisotropic model, in the short term. In the long term this difference diminishes, which means that during consolidation the isotropic model results in higher swelling than the anisotropic model. Although this is contrary to the softer drained response of the anisotropic model in oedometer swelling, it can be explained by considering the effective stress paths and pore pressure generation developed during undrained excavation. The stress path behind the wall is one of compression with the horizontal stress reducing. Figure 5 shows the total stress path for a corresponding triaxial test; the effective stress path for this test is the same as for test A3 38.7m. In this case, the isotropic model generates higher suctions than the anisotropic model. This is also evident in the retaining wall problem when the pore water pressure contours generated behind the wall in the short term are examined. Therefore, as the final long term pore pressures are similar for both models, the isotropic model results in higher swelling during the consolidation stage. Similar trends can be observed for case 3, albeit with smaller magnitudes due to the stiffer support system.

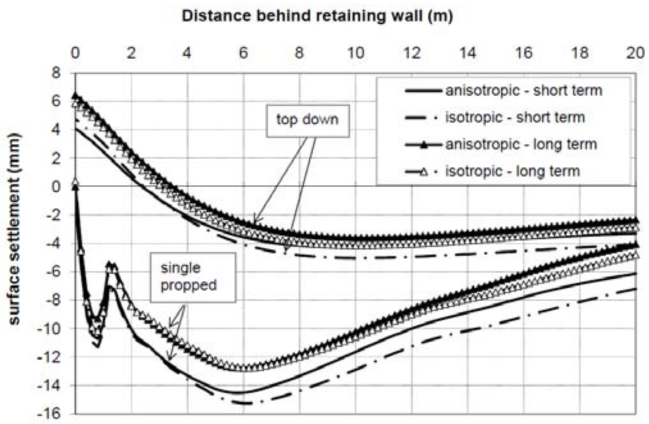

Figure 4. Surface settlement profile behind wall for cases 1 and 3.

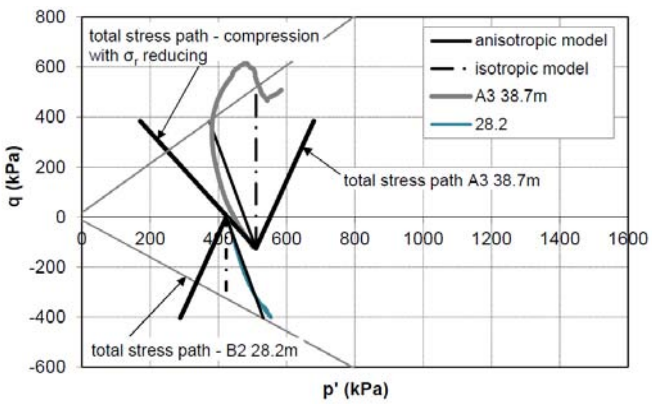

Figure 5. Stress path for an undrained triaxial extension test from the T5 research (test data from Hight et al. 2007).

Figure 6 shows the heave predicted at the base of the excavation for case 1. In the short term, the isotropic model predicts more heave, than the anisotropic model. During this stage of the analysis the stress path underneath the excavation is an extension path with reducing vertical stress. A corresponding undrained triaxial extension test from the T5 research (test 28.2), together with the simulations of the two models is shown in Figure 5. In this case the anisotropic model develops higher suctions than the isotropic model. This is confirmed in Figure 7a which shows the pore pressures below the base of the excavation for case 1. As the pore pressures in the long term are practically the same, one would expect that during the consolidation stage the anisotropic model would predict more swelling, especially as it shows a softer drained response in oedometer simulations.

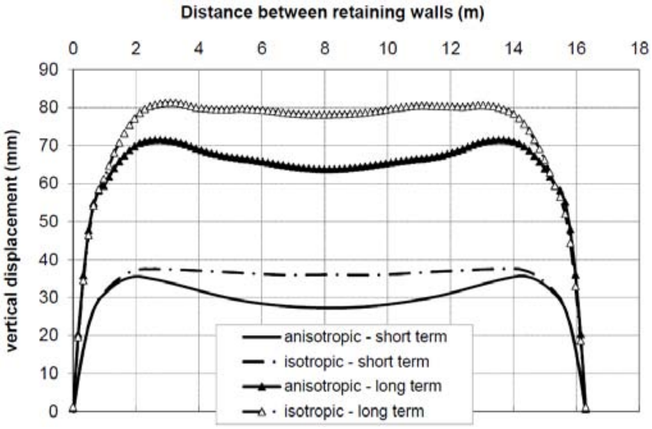

Figure 6. Basement heave for case 1.

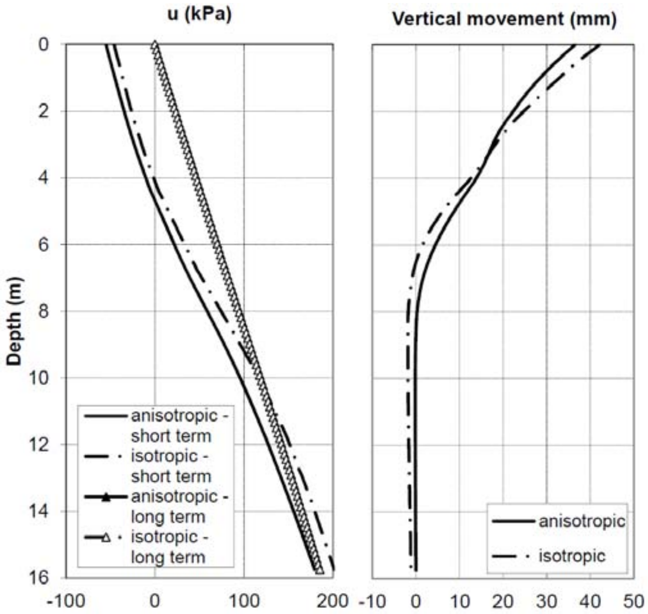

Figure 7. a) Pore pressures b) Vertical movements below base of excavation in the middle of the excavation for case 1

However, Figure 6 shows that this is not the case, i.e. the isotropic model results in higher swelling during the consolidation stage. Figure 7b shows the vertical movement developed only during the consolidation stage in the middle of the excavation plotted against depth below the base of the excavation for the single propped wall. This shows that with the anisotropic model there is more swelling than with the isotropic model at depths below 4m; however the isotropic model swells more at shallower depths. This does not agree with the fact that the anisotropic model develops higher suctions but can be explained by the fact that in the area below the base of the excavation plasticity has been invoked, with the yield surface being reached earlier in the case of the isotropic model (see Figure 5).

5 SUMMARY AND CONCLUSIONS

This study examines the effect of stiffness anisotropy on the behaviour of a deep excavation in a stiff plastic clay. The predictions of a cross anisotropic nonlinear elasto-plastic model are compared with those of an isotropic model which has been used extensively in the past. Three propping systems have been examined; a single-propped, a double-propped and a multi-propped wall. In relation to the effects of stiffness anisotropy, the study has shown that:

- In the short term, the anisotropic model predicts 9 – 15% smaller movements than the isotropic model, depending on the propping system. For the stiff support system the predictions obtained with the anisotropic model agree well with measured wall movements.
- In the long term, anisotropy does not affect wall movements further as they remain largely unaltered, due to a stiff permanent support system.
- Soil stiffness anisotropy has a smaller effect on wall movements than the propping system.
- In the short term, the anisotropic model predicts smaller heave at the base of the excavation and generally smaller settlements behind the wall.
- In the long term, movements below and around the excavation are governed by the different stress paths and associated pore pressure generation predicted by the two models during undrained excavation and loading. It has also been demonstrated that plasticity, which may be invoked at different stages for the different models, can play an important role.

This paper demonstrates that there are many facets associated with the modelling of stiffness anisotropy that influence predictions, including the stress path and associated pore pressure changes. The latter can be particularly influential when considering conditions in the long term.

REFERENCES

Franzius, J.N. Potts, D.M. & Burland, J.B. 2005. The influence of soil anisotropy and Ko on ground surface movements resulting from tunnel excavation, *Geotechnique* **55**, No. 3, 189–199.

Gaba, A.R. Simpson, B. Powrie W. & Beadman D.R (2003). *Embedded Retaining Walls: Guidance for Economic Design*. Construction Industry Research and Information Association, CIRIA C580.

Gasparre, A. Nishimura, S. Minh, N.A. Coop, M.R. & Jardine, R.J. 2007. The stiffness of natural London Clay, *Geotechnique* **57**, No. 1, 33–47.

Graham, J. & Houlsby, G.T. 1983. Anisotropic elasticity of a natural clay, *Geotechnique* **33**, No. 2, 165–180.

Grammatikopoulou, A. Schroeder, F.C. Kovacevic, N. Germano, V. & Gasparre, A. 2011. The influence of stiffness anisotropy on the behaviour of a stiff natural clay, *Proceedings of the 15th European Conference on Soil Mechanics and Geotechnical Engineering* (Eds. Anagnostopoulos, A. Pachakis, M. Tsatsanifos, C.), Athens, IOS Press, 1, 545–550.

Hight, D.W. & Higgins, K.G. 1995. An approach to the prediction of ground movements in engineering practice: background and application. *Proc. of the Intern. Symposium on Pre-failure Deformation of Geomaterials*, Sapporo, A.A. Balkema, Rotterdam, 1995, 909-945.

Hight, D.W. Gasparre, A. Nishimura, S. Minh, N.A. Jardine, R.J. & Coop, M.R. 2007. Characteristics of the London Clay from the Terminal 5 site at Heathrow Airport, *Geotechnique* **57**, No. 1, 3–18.

Jardine, R.J. Potts, D.M. Fourie, A.B. & Burland, J.B. 1986. Studies of the influence of non-linear stress-strain characteristics in soil-structure interaction, *Geotechnique* **36**, No. 3, 377–396.

Jardine, R.J. Potts, D.M. St John, H.D. & Hight, D.W. 1991. Some practical applications of a non-linear ground model, *Proceedings of the 10th European Conference on Soil Mechanics and Foundation Engineering*, Florence, 1, 377–396.

Jurecic, N. Zdravkovic, L. Jovicic, V. 2012. Predicting ground movements in London Clay. *Proceedings of the Institution of Civil Engineers - Geotechnical Engineering* **166**, No. 5, 462-482.

Lings, M.L. Pennington, D.S. & Nash, D.F. 2000. Anisotropic stiffness parameters and their measurement in a stiff natural clay, *Geotechnique* **50**, No. 2, 109–125.

Potts, D.M. & Zdravkovic, L. 1999. *Finite element analysis in geotechnical engineering: Theory*, Thomas Telford, London.

St John, H.D. Potts, D. M. Jardine, R. J. & Higgins, K. G. 1993. Prediction and performance of ground response due to construction of a deep basement at 60 Victoria Embankment. *Predictive Soil Mechanics – Proceedings of the Wroth Memorial Symposium*, Oxford, July 1992, Thomas Telford, London, 581–607.

Analysis of strip foundation performance on liquefied ground with limited ground improvement

Analyse du comportement des foundations superficielles sur du sol liquefiable après l'amelioration du sol limitée

V. Dimitriadi and G.D. Bouckovalas

ABSTRACT According to modern seismic codes, the use of shallow foundations on liquefiable soils is only acceptable after proper ground improvement underneath and around the foundation. Still, there are no widely acceptable guidelines for choosing the required thickness and extent of the improved ground, as well as for computing foundation settlements. This problem is investigated herein numerically, through fully coupled non-linear 2-D analyses with the Finite Difference code FLAC, using the Critical State Plasticity constitutive model NTUA-SAND [Andrianopoulos et al. (2010)] to simulate the cyclic response and liquefaction of the sand. The parametric investigation initially focuses upon the reference case of ground improvement with "infinite" lateral extent (the improved zone extends to the lateral grid boundaries). Subsequently, the width of ground improvement (Limp) is progressively reduced to nearly the width of the footing itself. The numerical predictions are organized into design charts and empirical relations, while conclusions are drawn regarding the optimum (from a cost-benefit point of view) extent of ground improvement.

1 INTRODUCTION

Seismic liquefaction leads to significant shear strength degradation of the foundation soil, as well as accumulation of dynamic settlements as well as to the temporary degradation of the bearing capacity of shallow foundations. Based on current practice, the liquefiable layer is bypassed with the use of piles, which transfer the structure loads to deeper and nonliquefiable strata. In addition, soil improvement is applied locally, to mitigate liquefaction and reduce the lateral loads applied upon the piles by the liquefied soil.

Experimental and theoretical studies have indicated that the existence of non-liquefiable soil strata (natural deposits or artificially created layers) on the ground surface may moderate the above liquefaction effects, to such an extent, that the use of shallow foundations becomes acceptable. Namely, Liu & Dobry (1997) examined the effect of the thickness of a top layer of non-liquefiable densified sand on the seismic response of a shallow foundation. Their results indicate significant reduction of seismic induced settlements, even when the specified layer did not extend to the entire thickness of the liquefiable layer.

Additionally, Naesgaard et al. (1998) and Karamitros et al. (2013a&b) have numerically investigated the problem of the seismic response of shallow foundations on such two-layered soil profiles, consisting of a clay layer underlain by liquefiable sand. The specific studies provide the theoretical background for the use of shallow foundations on liquefiable ground, while simple analytical relationships are proposed for the evaluation of the seismic settlements and the degraded post-shaking bearing capacity of the foundation.

The present paper focuses on the case where the non-liquefiable top layer is artificially created; using deep dynamic compaction and gravel drains and has finite dimensions, (depth and width) around the shallow foundation. The problem is numerically investigated, through fully coupled non-linear 2-D analyses, while emphasis is given to the effect of spatially limited ground improvement on foundation settlements.

2 NUMERICAL ANALYSES

The investigation of the seismic response of the shallow foundation on liquefiable soil with controlled ground improvement was performed through numerical analyses with the Finite Difference Code FLAC and the arrangement presented in Figure 1. The basic assumptions of the numerical methodology (constitutive model, boundary conditions, soil permeability) as well as the verification of its accuracy against centrifuge test results are outlined in Dimitriadi (2014) and will not be repeated here. It is only briefly mentioned that the simulation of the shallow foundation was considered rigid, whereas the grid size and its discretization were determined following sensitivity analyses.

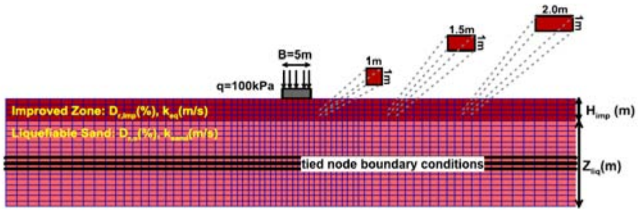

Figure 1. Used grid configuration in the 2-D numerical analyses

The top improved layer was considered uniform with equivalent properties (relative density and permeability), corresponding to a grid of gravel drains with replacement ratio α_s. For the evaluation of its equivalent properties, a set of 72 parametric numerical analyses of free field response was initially performed for three different depths of improvement, i.e. H_{imp}=4, 6 & 8m, replacement ratio values α_s = 0 ÷ 0.20 and initial relative density of the natural soil $D_{r,o}$ = 35 ÷ 70%. The numerical results are summarized in Figure 2 for the common case of maximum allowable excess pore pressure ratio within the improved layer, i.e. $r_{u,max}$ = 0.40.

The numerical analyses of footing response were performed in three distinct stages: (a) initial geostatic stresses are generated and the foundation load under static conditions is incrementally applied up to the desired contact pressure q, (b) a fully coupled effective stress dynamic analysis with parallel water flow is executed, subjecting the soil-foundation system into a harmonic seismic excitation. During this stage, excess pore pressures develop and seismic settlements accumulate under constant value of the average foundation contact pressure. (c) Upon the end of the shaking, and while the soil is still under a liquefied state, the contact pressure of the foundation is gradually increased until bearing capacity failure.

The seismic response of the shallow foundation is initially evaluated for the two-layered soil profile shown in Figure 1, which corresponds to reference conditions of "infinite" improvement width. A set of 84 numerical analyses was executed to examine the effect of soil [relative density D_r(%), natural soil permeability k_{sand}(m/s), thickness of improved layer H_{imp}(m)], excitation [maximum acceleration a_{max}(g), period T_{exc}(s) and number of loading cycles N] as well as footing properties [width B(m) and contact pressure q(kPa)]. The effect of the lateral extent of the improved zone around the footing was examined separately, through a set of 96 numerical analyses, in which the width of the improved zone was reduced progressively up to the width of the footing itself.

3 SEISMIC SETTLEMENTS

As thoroughly explained by Karamitros et al. (2013), the accumulation of dynamic settlements of the shallow foundation, is not the result of the dynamic compaction of sand, but rather the outcome of recurrent failures of the foundation soil, in the sense of a Newmark type sliding block

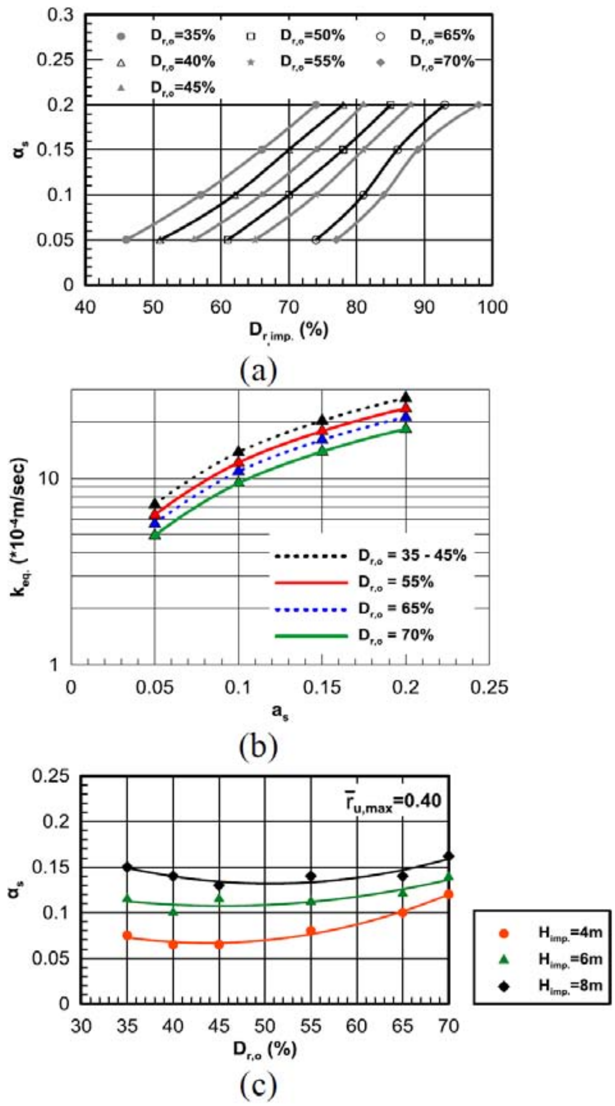

Figure 2. Charts for the computation of equivalent (uniform) properties for the improved zone, for $r_{u,max}$=0.40, in terms of initial relative density $D_{r,o}$(%) and the depth of improvement H_{imp}(m).

mechanism. More specifically, at the time of the maximum acceleration occurrence at each direction, a one-sided wedge-type failure mechanism develops at the opposite direction of the applied motion, as a result of the inertia forces acting upon the foundation and the soil. The specific mechanism is activated twice during one full loading cycle and leads to the incremental accumulation of two vertical displacement components. The associated horizontal displacements develop in opposite directions and practically delete one another.

Based on the above mechanism it turns out that dynamic settlements are proportional to the excitation characteristics and in particular the composite term:

$$\rho_o = \frac{v_{max}^{\ 2}}{\alpha_{max}} N = \alpha_{max} T^2 N \qquad (1)$$

where v_{max}^2 the maximum applied velocity, α_{max} the maximum acceleration, T is the excitation period, N the number of significant loading cycles of the applied excitation.

The effect on seismic settlements of the remaining parameters, which are not incorporated in the ρ_o term, is examined in Figure 3, parallel to their effects on the degraded bearing capacity factor of safety $F.S._{deg}$.

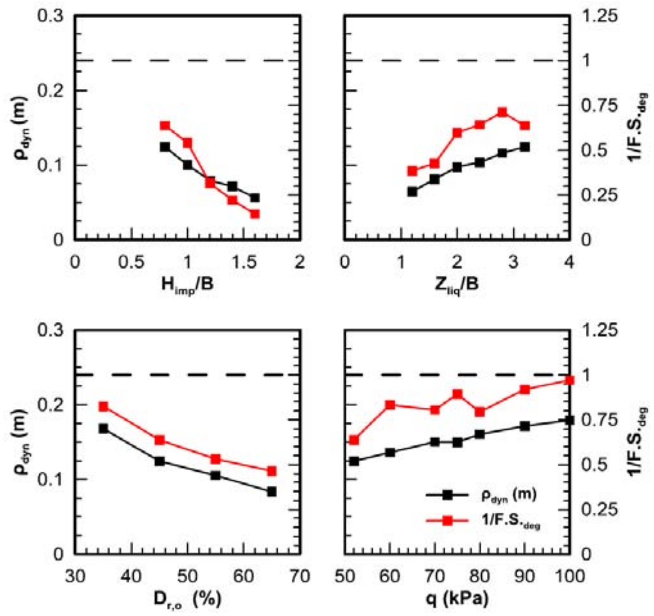

Figure 3. Effect of independent problem parameters on dynamic settlements and the inverse of the degraded safety factor $1/FS_{deg}$.

This parallel evaluation leads to the following key observation: the examined parameters have qualitatively the same effect on the dynamic settlements and on the inverse of the degraded factor of safety $1/F.S._{deg}$. Hence, their effect can be incorporated in the latter, and the analytical relation for the computation of seismic settlements is simplified to:

$$\rho_{dyn} = 0.019\alpha_{max}\left(T_{exc} + 0.63T_{soil}\right)^2 N\left(\frac{1}{F.S._{deg}^{\ inf}}\right)^{0.45} \left[1+0.25\left(\frac{1}{F.S._{deg}^{\ inf}}\right)^{4.5}\right] \qquad (2)$$

In the above equation, T_{soil} is the elastic period of the soil column, which was introduced in the analytical expression, to account for the effect of the soil column in the propagation of the seismic motion from the base – where it was initially applied – to the ground surface, where the foundation settlements accumulate.

The accuracy of the proposed analytical expression is evaluated in Figure 4a and 4b, on a one-to-one basis between the analytical predictions and the numerical results. It is observed that 84% of the analytical predictions lay between ±25% of the numerical results. The relative error of the analytical predictions is limited to approximately ±20%, with a standard deviation equal to 21%.

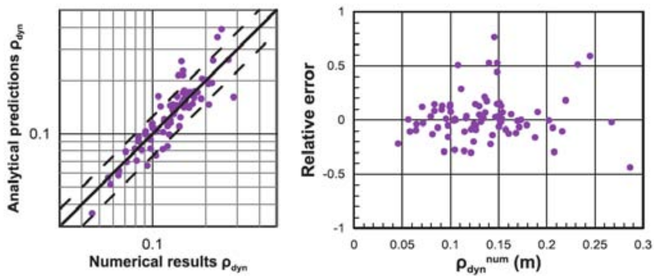

(a) (b)

Figure 4. (a) Comparison between numerical results and analytical predictions, (b) relative error against numerical results.

4 DEGRADED BEARING CAPACITY

The onset of liquefaction leads to a temporary but significant degradation of the static bearing capacity of the foundation soil, which lasts from the end of shaking, until the complete dissipation of the earthquake generated excess pore water pressures. The corresponding failure mechanism draws upon that proposed by Meyerhoff & Hanna (1978) for static failure of shallow foundations resting upon twolayered soil profiles (Figure 5): punching of the foundation through the improved top layer, followed by a generalized wedge-type failure within the liquefiable sand layer. A basic deviation of the conventional Meyerhoff & Hanna static failure mechanism is due to the dissipation of the earthquake-induced excess pore pressures, from the liquefiable sand towards the much more permeable improved top layer. As a result, a transition zone of partially liquefiable sand, contributes to the shear strength of the top improved layer.

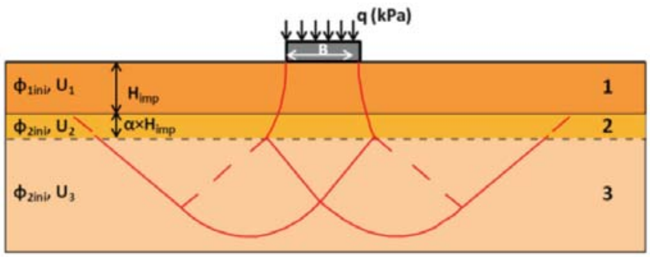

Figure 5. Failure mechanism of shallow foundation: (1) improved zone, (2) transition zone of partially liquefied ground (3) liquefied ground.

Based on the above, the analytical expression proposed by Meyerhoff & Hanna (1978) is modified as follows to account for the specific problem conditions:

$$
\begin{aligned}
q_{ult,deg} &= \gamma' H_1^{\,2} K_s \frac{\tan\phi_{1,deg}}{B} + \\
&+ \gamma' \cdot [(1+\alpha)^2 - 1] \cdot H_1^{\,2} K_s \frac{\tan\phi_{2,deg}}{B} - \\
&- \gamma'(1+\alpha) H_1 + \frac{1}{2}\gamma' B N_{\gamma 3} + \gamma'(1+\alpha) H_1 N_{q3}
\end{aligned} \tag{3}
$$

where

$$
\begin{aligned}
N_{q,i} &= \tan^2\left(45 + \frac{\varphi_{i,deg}}{2}\right) e^{\pi \tan\varphi_{i,deg}} \\
N_{\gamma,i} &= 2(N_{q,i} + 1)\tan\varphi_{i,deg}
\end{aligned} \tag{4}
$$

The degraded values of friction angle ($\varphi_{i,deg}$) in the above Equations (3) & (4), are estimated based on the initial value of the sand's friction angle ($\varphi_{i,o}$) and the corresponding excess pore pressure ratio at the end of shaking U_i, as:

$$\tan\varphi_{i,deg} = (1 - U_i)\tan\varphi_{i,o} \tag{5}$$

The remaining parameters in Eqs. (3) to (5) are estimated as follows:

Coefficient α: relates to the thickness of the transition zone and is expressed as a percentage of the improvement depth. It is expressed as a function of the equivalent permeability of the improved zone k_{eq} (m/s), the period of the shaking T (s), the number of the significant loading cycles N, as well as the thickness of the improved zone H_{imp} (m):

$$\alpha = 3.76\left[\frac{k_{eq} T N}{H_{imp}}\right]^{0.256} \tag{6}$$

Excess pore pressure ratio U_i (i=1,2 & 3): U_1 represents the excess pore pressure within the improved allowable value considered in the design stage i.e. $U_1 = 0.54*U_{design}$. U_2, represents the average excess pore pressure ratio within the transition zone, in the free field, and is defined as $(1+U_1)/2$. Finally, U_3 corresponds to the liquefied ground, underneath the foundation, below the improved and the transition zones. It is expressed as a function of the degraded bearing capacity q_{ult}^{deg}:

$$U_3 = 0.86\left(\frac{q_{ultdeg}^{\;inf}}{p_\alpha}\right)^{-0.18} \le 1.00 \tag{7}$$

Coefficient K_s: is used to compute the shear strength across the partially liquefied improved and transitional soil zones, below the edges of the foundation. It is expressed as a function of the applied contact pressure of the foundation q(kPa), the thickness of the improved zone H_{imp}(m), and the width of the foundation B(m):

$$K_s = 1.00\left(\frac{q}{p_\alpha}\right)^{-0.30}\left(\frac{H_{imp}}{B}\right)^{-0.50} \tag{8}$$

Ultimately, the degraded factor of safety for conditions of "infinite" improvement ($F.S._{deg}^{inf}$) is evaluated from Equation (9), as a function of the nominal value of the factor of safety ($F.S._{deg}^{inf*}$) corresponding to the q_{ult}:

$$F.S._{deg}^{\;inf} = \frac{F.S._{deg}^{\;inf*}}{0.05 + 0.60\left(F.S._{deg}^{\;inf*}\right)^{0.85}} > 0.60 F.S._{deg}^{\;inf*} \tag{9}$$

The accuracy of the proposed analytical relation for the evaluation of the degraded factor of safety is evaluated in Figure 6, both on a one-to-one basis between the analytical predictions and the numerical results, as well as in terms of relative error. It is thus observed that approximately 80% of the analytical predictions lay between ±25% from the numerical results, with a standard deviation of the relative error equal to 25%.

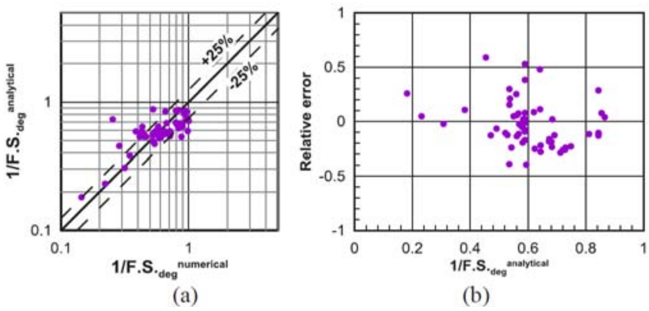

Figure 6. (a) Comparison between numerical results and analytical predictions, (b) relative error against numerical results.

5 EFFECT OF IMPROVEMENT WIDTH

The previous analytical expressions for the evaluation of dynamic settlements and the degraded bearing capacity of the foundation are valid for a large, theoretically infinite, horizontal extent of the improved zone. The statistical processing of the second set of numerical analyses, for limited extent of ground improvement, led to the correction of the analytical expressions described previously, in order to take into account the finite width of the improved zone L_{imp} (Dimitriadi 2014). Hence, seismic settlements may be computed from the following Equation (10),

$$\rho_{dyn} = \rho_{inf} \Big/ \left[1 - \exp\left(-1.05\left(\frac{H_{imp}}{B}\right)^{-1}\left(\frac{L_{imp}}{B}\right)^{0.30}\right)\right] \tag{10}$$

while the degraded factor of safety F.S.$_{deg}$ may be computed from iterative solution of the following non-linear Equation (11):

$$\left(\frac{F.S._{deg}}{F.S._{deg}^{\ inf}}\right)^{-0.45} = \left\{1-\exp\left[-1.05\left(\frac{H_{imp}}{B}\right)^{-1}\left(\frac{L_{imp}}{B}\right)^{0.30}\right]\right\}\times$$
$$\times\frac{\left(F.S._{deg}^{\ inf}\right)^{4.5}+0.25\left(\frac{F.S._{deg}}{F.S._{deg}^{\ inf}}\right)^{4.5}}{\left(F.S._{deg}^{\ inf}\right)^{4.5}+0.25} \qquad (11)$$

Note that the above effects are expressed in terms of the dimensions of the improved zone normalized against the width of the foundation B(m). Hence, it was considered practical to relate the size of ground improvement with the volume of the improved area V_{imp}, defined (for 2-D conditions) as the product between the width and the thickness of the improved area. The new relations for the computation of the seismic settlements and degraded bearing capacity are presented graphically in Figure 7. The red line in Figure 7 sets the limit beyond which, further increase of the improved area renders a rate of variation less than 5%, leading to a high cost-benefit ratio. Based on the above criterion, it turns out that the maximum benefit from the use of the proposed methodology is obtained for improvement depths between 0.5 ÷ 2 times the width of the foundation B and improvement width between 2 ÷ 3.5 the width of the foundation B.

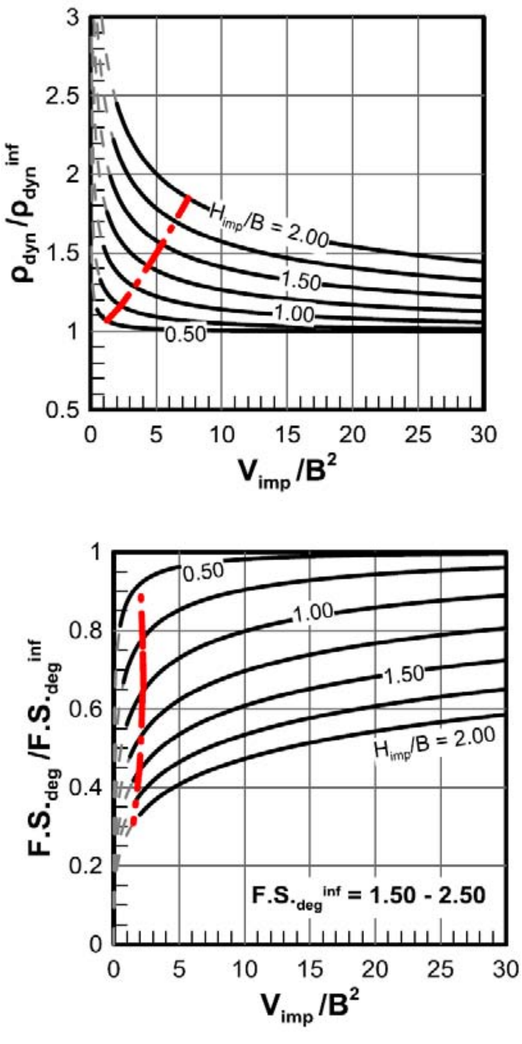

Figure 7. Charts for dynamic settlement and degraded factor of safety computation in the case of ground improvement with limited lateral dimensions.

6 CONCLUDING REMARKS

The problem of spatially limited ground improvement on foundation settlements is numerically investigated herein and an analytical methodology is proposed. Based on this, independently of the thickness of the improved zone, gradual reduction of its lateral extent increases the seismic settlements accumulation and drastically reduces the post-shaking degraded bearing capacity of the foundation. Optimum results from the use of the methodology are obtained for improvement depths between 0.5 ÷ 2 and improvement width between 2 ÷ 3.5 times the width of the foundation B. Further consideration is given to a more accurate evaluation of the degraded bearing capacity, given that the soil liquefaction leads to very sot soil conditions that favor the development of local failure of the soil underneath the improved crust.

The specific criteria and the analytical methodology presented herein have been developed for shallow strip foundations. Their expansion for the description of the seismic response of rectangular foundations is currently under way.

ACKNOWLEDGEMENTS

This research has been co-financed by the European Union (European Social Fund – ESF) and Greek national funds through the Operational Program "Education and Lifelong Learning" of the National Strategic Reference Framework (NSRF) - Research Funding Program: THALES. Investing in knowledge society through the European Social Fund.

REFERENCES

Adalier, K. Elgamal, A. Meneses, J. Baez, J.I. 2003. Stone columns as liquefaction countermeasure in non-plastic silty soils, *Soil Dynamics and Earthquake Engineering*, **23,** 571-584.

Dimitriadi, V. 2014. Performance based design and soil improvement methods of shallow foundations on liquefiable soils, *PhD Thesis*, NTUA

Karamitros, D. K. Bouckovalas, G.D. Chaloulos, Y.K. 2013. Insight into the seismic liquefaction performance of shallow foundations, *Journal of Geotechnical and Geoenvironmental Engineering*, **139**, 599-607.

Karamitros, D. K. Bouckovalas, G.D. Chaloulos, Y.K. 2013. Seismic settlements of shallow foundations on liquefiable soil with a clay crust, *Soil Dynamics and Earthquake Engineering*, **46**, 64-76.

Karamitros, D. K. Bouckovalas, G.D. Chaloulos, Y.K. Andrianopoulos, K.I. 2013. Numerical analysis of liquefaction-induced bearing capacity degradation of shallow foundations on a two-layered soil profile, *Soil Dynamics and Earthquake Engineering*, **44**, 90-101.

Liu, L. Dobry, R. 1997. Seismic response of shallow foundation on liquefiable sand, *Journal of Geotechnical and Geoenvironmental Engineering*, **123,** 557-567.

Meyerhof. G.G. Hanna, A.M. 1978. Ultimate bearing capacity of foundations on layered soils under inclined load, *Canadian Geotechnical Journal*, **15**, 565 – 572.

Naesgaard, E. Byrne, P.M. Ven Huizen, G. 1998. Behaviour of light structures founded on soil 'crust' over liquefied ground, *Geotechnical Earthquake Engineering and Soil Dynamics III, Proceedings of a Specialty Conference*, **1**, 422-434.

Numerical analysis of liquefaction affected shallow foundations performance on improved ground

Analyse numérique du comportment des fondations superficielles sur du sol amélioré contre la manifestation de la liquefaction

V. Dimitriadi, G.D. Bouckovalas and Y. Chaloulos

ABSTRACT A novel numerical methodology is presented and used to simulate the seismic response of footings on liquefiable ground, locally improved in order to reduce settlements and increase the bearing capacity of the foundation. The numerical simulation adopts the nonlinear Finite Difference code FLAC-3D (v.4.0), combined with the NTUA Sand constitutive model, which has been developed at the Foundation Engineering Laboratory of NTUA in order to predict the cyclic response and liquefaction resistance of sands, on the basis of Critical State soil plasticity. The proposed methodology is evaluated through comparative application to the well documented centrifuge experiments of Liu & Dobry (1997).

1 INTRODUCTION

The beneficial effect of a non-liquefiable soil layer at the ground surface for the reduction of liquefaction induced foundation settlements and the prevention of bearing capacity failure has been historically documented through field observations and case histories, such as in the Dagupan earthquake (1990). Acacio et al. (2001) used published data for the specific event, in combination with previously published historical data by Ishihara (1985), and managed to relate the occurrence of shallow foundation bearing capacity failure to the thickness of the non-liquefiable surface crust. In addition to field case histories, pioneering experimental studies have studied the particular problem and have described the highly non-linear governing mechanisms and the results of the liquefied soil – foundation interaction.

Liu & Dobry (1997) were the first to experimentally study the performance of shallow foundations on liquefiable ground with controlled ground improvement. In more detail, they performed two independent series of centrifuge tests, one on improved ground and the second on the natural ground. The purpose of the first series of tests was to evaluate the effect of improved ground thickness on the foundation performance, while the second series focused upon the associated effects of soil permeability.

Adalier et al. (2003) examined the seismic response of a liquefiable silt layer, improved with gravel drains, focusing on the stiffness increase of the improved zone under free field conditions as well as under the presence of a shallow foundation. More recently, Dashti et al. (2010) examined the seismic response of different structural systems, founded by means of a stiff mat foundation on soil profiles including a shallow, thin liquefiable layer.

In parallel to centrifuge experiments, dynamic non-linear effective stress numerical analyses are gaining ground for the simulation of such complex problems and tend to become an alternative, cost efficient method of analysis and design. For instance, Naesgaard et al. (1998) investigated numerically the seismic response of light shallow foundations on liquefiable ground, overlain by a non-liquefiable clay crust. More recently, similar numerical simulations were performed by Karamitros et al. (2013), which led to the formulation of an analytical methodology for the performance – based design of shallow foundations, allowing the computation of seismic settlements, as well as, post-shaking bearing capacity degradation.

In the above context, the present paper describes a numerical methodology for the simulation of the seismic response of shallow foundations on liquefiable ground with limited (in extend) ground improvement. The numerical simulation is performed with the Finite Difference Code FLAC-3D. The seismic response and the liquefaction resistance of the sand are simulated with the NTUA-SAND constitutive model, which was implemented to FLAC-3D by Andrianopoulos et al. (2010). The overall accuracy of the numerical methodology is evaluated against the well-established set of centrifuge test results of Liu & Dobry (1997) mentioned above.

2 CENTRIGUGE EXPERIMENTS

Verification of the proposed numerical methodology will be based on the first set of centrifuge experiments performed by Liu & Dobry (1997), which is more relevant to actual applications. The particular set consists of five experiments, which examine the effect of the thickness of vibro-compacted liquefied sand on the seismic response of a shallow foundation resting upon it. The purpose of the experiments is to investigate the mechanism behind the development of seismic settlements, as well as to evaluate the response of the soil-foundation system in terms of acceleration amplification, as well as excess pore pressure built up and foundation settlement.

The model configuration is presented in Figure 1. It consists of a circular shallow foundation of diameter B, on top of a liquefiable (saturated) sand layer, compacted within a specified area, around the foundation, of width 1.6B and different depths Z_c. The soil and foundation response was measured with the aid of seven pore pressure transducers (PF, PC and PE), two accelerometers (a_f and a_s) and two LVDTs (S_c and S_f). The above model was build in a rigid rectangular bucket of model size 454×204×241mm^3, which was subjected to 80g centrifugal acceleration.

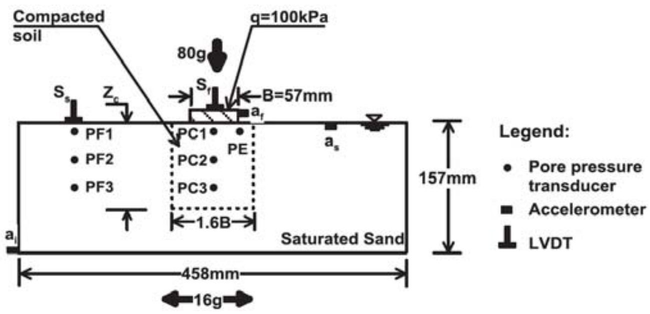

Figure 1. Model configuration and instrumentation of Liu & Dobry (1997) test series.

The liquefiable soil used in all tests is a fine, uniform Nevada #120 sand with initial relative density equal to D_r = 52±3% and a total thickness equal to 12.5m in prototype scale. The reported relative density of the improved sand in all tests is on average equal to D_{rimp} =90%.

The properties of the natural and the compacted soil are summarized in Table 1. In the reference test (C_0) the foundation is in direct contact to the liquefiable ground. In the four remaining tests, the width of the compacted zone, around the foundation, remained constant, and the depth of densification ranged from 0.7 to 2.8 times the diameter of the footing, eventually covering the entire thickness of the liquefiable layer. A harmonic seismic excitation, of frequency equal to f=1.5Hz and maximum acceleration equal to 0.2g (Figure 2), was applied at the base of the centrifuge container.

Figure 3 shows the accumulated seismic settlements and the ratio of the maximum acceleration acting upon the foundation to the applied acceleration at the base of the rigid box, for the different normalized depths of the performed improvement Z_c/B. The beneficial effect of the compacted zone upon the reduction of the observed seismic settlements becomes evident from Figure 3a, as a reduction of about 60% is observed between the reference case and the case where the compacted zone covers the entire thickness of the liquefiable layer, i.e. Z_c=2.8B. However, Figure 3b reveals a parallel detrimental effect of ground improvement. Namely, it is shown that the improvement of the entire thickness of the liquefiable layer leads to the amplification of the seismic acceleration acting upon the foundation.

Table 1. Soil properties and densification depths Z_c

Test	Drini (%)	Dr,c (%)	Zc (m)	Zc/B
C_0	54	-	0	0
C_1	51	>100	3.22	0.71
C_2	55	88	6.72	1.47
C_3	49	91	9.45	2.07
C_4	51	89	12.5	2.76

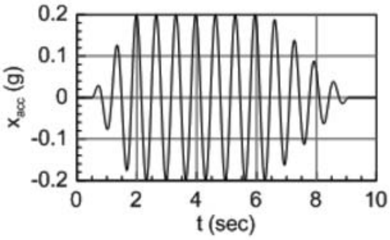

Figure 2. Harmonic excitation applied at the base of the configuration

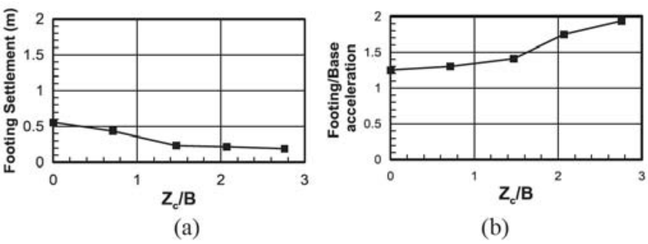

Figure 3. Experimental results of (a) dynamic settlements and (b) ratio of footing/base acceleration [Liu & Dobry (1997)].

3 NUMERICAL METHODOLOGY

The above centrifuge tests were simulated numerically with the FLAC 3D, a Finite Difference code, which allows the execution of fully coupled effective stress dynamic analyses with parallel water flow. Furthermore, it allows the inclusion of user-defined sophisticated constitutive models for the detailed description of the soil element response. In the present study, the cyclic response of the saturated sand was simulated with the NTUA-Sand constitutive model (Papadimitriou and Bouckovalas 2002, Andrianopoulos et al. 2010, Karamitros, 2010). This model is based on the Critical State Theory of soils and has been calibrated against laboratory cyclic and liquefaction test results on Nevada sand, i.e. the same sand that has been used in the centrifuge tests.

The geometric characteristics of the numerical model, shown in Figure 4, were closely adjusted to the prototype dimensions of the experimental configuration. Hence, the container's dimensions under a centrifugal acceleration of 80g correspond to prototype dimensions of 36.80×16×12.5 m^3, whereas the shallow stiff foundation measures a diameter of 4.56m and applies an average contact pressure equal to q=100kPa.

To take advantage of the system's symmetrical response along the y-direction, only half the footing was modeled by generating a 36.80×8×12.5m^3 grid, discretized into 11,500 brick zones with dimensions of 0.8×0.8×0.5m_3. The stiff shallow foundation is simulated with shell elements and it is square in shape, of equivalent area and average contact pressure (B=4.56m and q=100kPa).

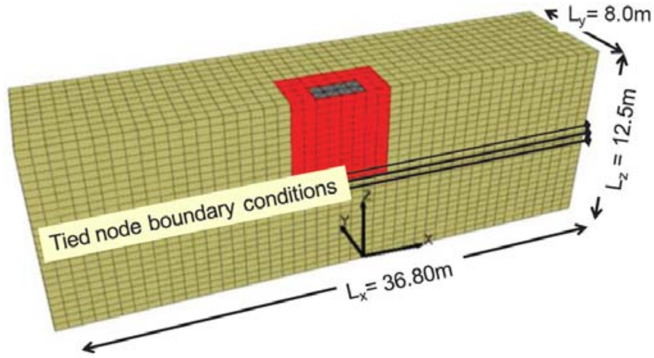

Figure 4. 3-D grid used in the numerical simulation of the centrifuge experiments

The loading sequence is divided in two stages: (i) generation of initial stresses and incremental application of the foundation's contact pressure, (ii) execution of a fully coupled dynamic analysis with parallel water flow, subjecting the system to the loading time history shown in Figure 2.

Boundary conditions were different between the two stages of loading. In particular, to describe the perfectly smooth inner walls of the container, horizontal displacements during the first stage of static loading are restrained in the lateral boundaries, whereas the bottom boundaries are restrained along the vertical direction. During the second stage of dynamic loading, tied-node boundary conditions were considered along the lateral boundaries of the configuration, which ensure the development of free field conditions, i.e. equal horizontal displacements at nodes of the same elevation. Vertical displacements are again restricted along the bottom boundary and the dynamic loading is applied horizontally – along the x-direction.

Based on laboratory tests of constant hydraulic height at 1g gravity conditions the coefficient of permeability for Nevada sand at D_r≈50% initial relative density is measured as k=0.0066cm/s (Arulmoli et al., 1992). However, Liu & Dobry (1997) propose to use the much lower value of k=0.0021cm/sec for seismic loading in order to account for the dynamic character of the applied loading and the continuous change in the direction of the pore fluid flow.

In addition to the previous suggestions for a constant value of the soil permeability coefficient, there are indications that the permeability of liquefiable soils is not constant during shaking but it increases as a function of the ever current excess pore pressure ratio r_u. Namely, Shahir et al. (2012) assumed that k increased from its initial value (i.e. for r_u=0), to an order of magnitude higher value at liquefaction (i.e. for r_u=1).

To investigate the above arguments, two sets of numerical analyses were performed, the first considering the initial "dynamic" value of the Nevada sand permeability k=0.0021 cm/s (Liu & Dobry 1997) and the second for the conventional (static) value of k=0.0066cm/s (Arulmoli et al., 1992), which is also equal to the logarithmic average between the values of dynamic permeability proposed by Shahir et al. (2012) for r_u= 0 and r_u=1.0. Additionally, given that the pore fluid, which was used in all five centrifuge tests, was water the above values were multiplied by the centrifugal acceleration (80g), leading to eighty times larger prototype values of fluid permeability (i.e. k=0.168cm/s and k=0.528cm/s) for each of the two groups of numerical analyses. Note that, at prototype scale, the above values correspond to the natural permeability coefficient of rather coarse sands.

4 EVALUATION OF NUMERICAL PREDICTIONS

4.1 Excess pore pressure generation

The numerical predictions are initially evaluated in terms of the excess pore pressure built up, for the reference case of liquefied ground without improvement. In particular, Figures 5a & 5b summarize the comparison between the experimental measurements (in black) and the numerical predictions for the two scenarios of the coefficient of the soil's permeability (with orange and green color). The comparison is performed at three different depths and two distinct positions, namely in the free field, away from the foundation (locations PC_1, PC_2 & PC_3 in Figure 1) and underneath the foundation (locations PF_1, PF_2 & PF_3 in Figure 1). In all cases there is a satisfactory agreement between the centrifuge recordings and the numerical predictions, both in terms of the maximum value of the developing excess pore pressure and the time of its occurrence. Additionally, this particular evaluation shows that the static value of the coefficient of permeability (orange line) captures slightly more accurately the evolution of the excess pore pressures with time.

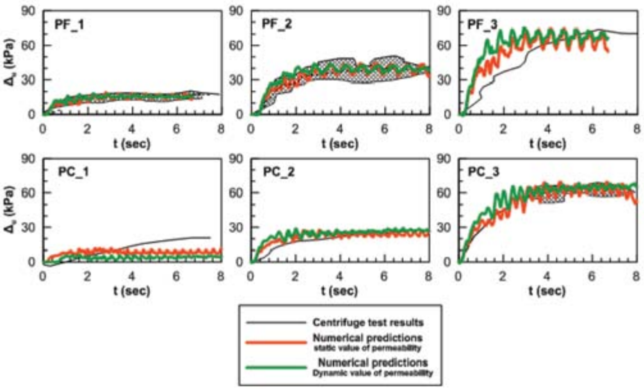

Figure 5. Excess pore pressure time histories Δu (kPa) in three different depths (a) in the free field and (b) underneath the footing.

4.2 Accumulation of seismic settlements

In the sequel, the proposed numerical methodology is evaluated in terms of seismic settlements. In particular, the numerical predictions for all five centrifuge tests are summarized in Figure 6, in terms of the normalized thickness of the compacted zone Z_c/B, for the two scenarios of permeability coefficient explained earlier.

It is observed that the numerical methodology predicts with sufficient (qualitative and quantitative) overall accuracy the beneficial effect of the compacted zone upon settlements. On average, best fit predictions are obtained for the dynamic value for the coefficient of permeability, while use of the static value consistently under-estimates settlements by about 20%. It is also of interest to observe that the benefits from the presence of the compacted zone are practically exhausted for improvement depths greater than about 1.5 times the width of the foundation B. This particular conclusion is verified by both the centrifuge test results and the numerical predictions.

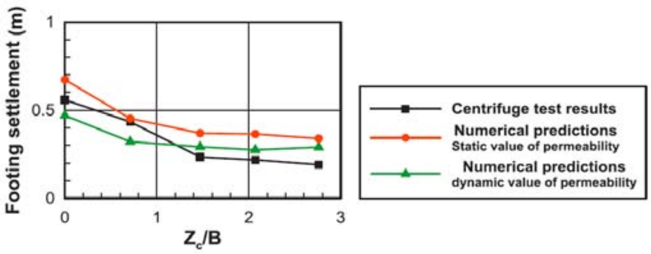

Figure 6. Footing settlement versus normalized densification depth Z_c/B.

The evaluation of numerical predictions regarding the amplification of the seismic acceleration applied to the footing, expressed as the footing/base acceleration ratio for different normalized improvement thicknesses, Z_c/B, is presented in Figure 7.

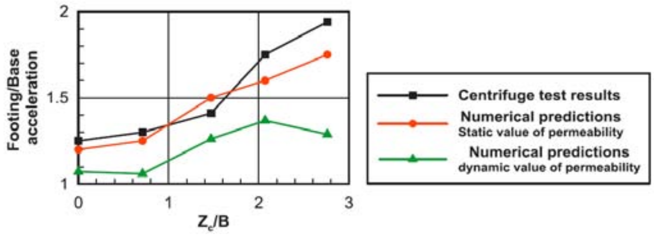

Figure 7. Footing/Base acceleration versus normalized densification depth Z_c/B.

Again, the agreement between the numerical predictions and the centrifuge test results is satisfactory, although now the static values of soil permeability provide best fit predictions, while the dynamic values provide a consistent lower bound. It is also interestingly noted that both sets of data indicate a steady increase of the amplification of the seismic motion acting upon the foundation with increasing depth of improvement. It is hence concluded that the extension of ground improvement to great depths, i.e. beyond 1.5B, is not beneficial, given that it may marginally contribute to the reduction of seismic settlements, but it will significantly amplify the seismic motion and the inertial forces acting upon the foundation and the super-structure.

5 SUMMARY AND CONCLUSIONS

The present paper deals with the numerical simulation of a rather complex problem of seismic foundation – soil interaction, under the extreme condition of subsoil liquefaction. The numerical methodology is initially outlined, and subsequently verified against experimental results from well documented centrifuge tests, aimed to explore the influence of localized ground improvement of liquefiable sand upon the seismic response of a circular shallow foundation (Liu & Dobry, 1997).

The comparison was performed in terms of (i) excess pore pressure generation, (ii) seismic settlements accumulation and (iii) footing/base acceleration ratio, for two possible scenarios regarding the value of soil's coefficient of permeability. It is thus concluded that:

(a) The numerical analyses predict with fairly good precision the beneficial effect of ground improvement on foundation settlement, but also its detrimental effect of seismic acceleration amplification at the footing and the super-structure.

(b) The static permeability coefficient provides the best overall fitting of the foundation response, as it may underestimate settlements by no more than 20% while it accurately predicts foundation accelerations.

(c) It is of practical interest that, the experiments, as well as the numerical analyses, show that the beneficial effect of ground improvement on settlements ceases for ground improvements depths larger than 1.5B (B is the diameter of the footing), while the amplification of footing acceleration increases steadily with the depth of improvement. Hence, it is not wise to extend ground improvement beyond that critical depth, as its net effect will become detrimental despite the associated cost increase.

ACKNOWLEDGEMENTS

This research has been co-financed by the European Union (European Social Fund – ESF) and Greek national funds through the Operational Program "Education and Lifelong Learning" of the National Strategic Reference Framework

(NSRF) - Research Funding Program: THALES. Investing in knowledge society through the European Social Fund.

REFERENCES

Acacio, A.A. Kobayashi, Y. Towhata, I. Bautista, R.T. Ishihara, K. 2001. Subsidence of building foundation resting upon liquefied subsoil case studies and assessment, *Soils and Foundations* **41**, 6, 111-128.

Adalier, K. Elgamal, A. Meneses, J. Baez, J.I. 2003. Stone columns as liquefaction countermeasure in non-plastic silty soils, *Soil Dynamics and Earthquake Engineering* **23**, 571-584.

Andrianopoulos, K.I. Papadimitriou, A.G. Bouckovalas, G.D. 2010. Explicit integration of bounding surface model for the analysis of earthquake soil liquefaction, *International Journal for Numerical and Analytical Methods in Geomechanics* **34**, 15, 1586–1614.

Arulmoli, K. Muraleetharan, K.K. Hosain, M.M. Fruth L.S. 1992. VELACS: verification of liquefaction analyses by centrifuge studies laboratory testing program soil data report, *Earth Technology Project* No.90-0562.

Chaloulos, Y.K. Bouckovalas, G.D. & Karamitros, D.K. 2013. Pile response in submerged lateral spreads: Common pitfalls of numerical and physical modeling techniques, *Soil Dynamics and Earthquake Engineering* **55**, 275–287.

Dashti, S. Bray, J.D. Pestana, J.M. Riemer, M. Wilson, D. 2010. Centrifuge testing to evaluate and mitigate liquefaction-induced building settlement mechanisms, *Journal of Geotechnical and Geoenvironmental Engineering* **136**, 7, 918-929.

Ishihara, K. 1985. Stability of natural deposits during earthquakes, *11th International Conference on Soil Mechanics and Foundation Engineering*, San Francisco, CRC Press.

Karamitros, D. K. Bouckovalas, G.D. Chaloulos, Y.K. 2013. Insight into the seismic liquefaction performance of shallow foundations, *Journal of Geotechnical and Geoenvironmental Engineering* **139**, 599-607.

Liu, L. Dobry, R. 1997. Seismic response of shallow foundation on liquefiable sand, *Journal of Geotechnical and Geoenvironmental Engineering*, **123**, 6, 557-567.

Naesgaard, E. Byrne, P.M. Ven Huizen, G. 1998. Behaviour of light structures founded on soil 'crust' over liquefied ground, *Geotechnical Earthquake Engineering and Soil Dynamics III, Proceedings of a Specialty Conference*, **1**, 422-434.

Papadimitriou, A. G. Bouckovalas, G. D. 2002. Plasticity model for sand under small and large cyclic strains: A multiaxial formulation, *Soil Dynamics and Earthquake Engineering*, **22**, 3, 191–204.

Shahir, H. Pak, A. Taiebat, M. Jeremic, B. 2012. Evaluation of variation of permeability in liquefiable soil under earthquake loading, *Computers & Geotechnics*, **40**, 74 – 88.

Experimental mechanics at the grain-scale in sand: Recent work from the geo-mechanics lab of Grenoble

Edward Andò, Gioacchino Viggiani and Jacques Desrues

Abstract

This paper presents some recent x-ray tomography work from Grenoble, illustrated with existing measurements of sand grain kinematics under triaxial compression, allowing full 3D kinematics to be measured for each grain over 18 scanned increments. Future challenges for the application of x-ray tomography in revealing other grain-scale processes in sand are also discussed.

***Keywords**: x-ray tomography; granular media; shear banding; discrete analysis*

1. Introduction

Continuum models of soil behaviour have long been used to describe the deformation characteristics of these materials, and with a good degree of success. Continuum models are easy to use directly within a Finite Element Model (FEM), allowing complex engineering problems to be simulated. The tendency of granular materials to undergo *strain localization* is difficult to capture with such models since the hypothesis of a continuum breaks down, as deformation structures emerge within the soil. Many experimental observations indicate that such structures (shear bands for example) have a characteristic size (width) of only a few grain diameters (regardless of grain size) – which indicates that this is a grain scale phenomenon. The modelling of such structures is understandably a fine art: continuum models need sophisticated techniques (such as enriched continua) to overcome Finite Element mesh dependency, whereas particle-based simulations such as the Discrete Element Method or Contact Dynamics require careful calibration. In any case, in order to be able to capture the behaviour of a granular medium undergoing localisation with a model, experimental observations at this scale are required.

This paper presents ongoing work from Laboratoire 3SR (Grenoble) on this very subject, where granular assemblies are deformed "*in-situ*" (*i.e.,* inside an x-ray tomography machine), allowing multiple states to be imaged in 3D. This is a technique which is getting increasing attention in materials science, and in the subject of the study of granular materials, the work of Alshibli (*e.g.,* Alshibli and Hasan, 2008) and the group at ANU (*e.g.,* Saadatfar *et al.,* 2013) must be mentioned. The paper shows existing work on the grain-scale study of shear banding, with results from triaxial testing, and a short discussion about future challenges.

2. Experimental setup

2.1 Materials and in-situ triaxial testing

This paper presents results obtained on an unsual material: Caicos ooids, a very rounded carbonate sand from the Turks and Caicos islands in the British West Indies, D50 = 420μm. These materials (along with others tested), are detailed fully in Andò (2013), Caicos ooids have been chosen in this case since their rounded shape helps the automatic identification of grains.

The triaxial tests used in this work differ significantly from standard ones to allow x-ray scanning of the specimen in various stages of deformation – to this end experiments are entirely performed within the Laboratoire 3SR x-ray microtomograph. Given that the D50 of the grains studied is in the order of 300μm, the pixel size necessary for sufficient information for grain has been set to 15.56 μm/px, meaning that an average particle will have around 20 pixels across a diameter (An average particle will therefore be composed of around 4200 3D pixels, known as voxels). This choice limits the field of view and consequently the size of the specimen is reduced to 22mm height and 11mm diameter. Despite this extreme miniaturisation, the specimen is composed of more than 50,000 grains of sand.

Furthermore, since x-ray tomography requires the rotation of the specimen, the steel tie bars that usually take the return force from the compression of the specimen would severely degrade the scan – to avoid this the pressure cell (which is made in x-ray transparent plexiglas or polycarbonate) takes this extra load. Specimens are prepared dense (through dry pluviation through a 1m tube), and are tested dry. This would normally mean that no volume changes can be measured, however these are obtained from the different 3D images. Triaxial testing is done under strain control at a strain rate of 0.1%/min, however loading is interrupted at various points during the test to scan the specimen (acquiring around a thousand radiographs as the specimen rotates through 360°). When loading is stopped the specimen relaxes – the majority of the relaxation happens in a few minutes after loading is stopped. Axial force and imposed displacement are measured externally.

2.2 Image-based measurements

The 3D images coming from each scan contain around 1000×1000×1600 voxels, each voxel representing a reconstructed value of x-ray attenuation (which is roughly related to density, meaning that grains have "high" and pores have "low" grey values). From such an image, a local field of porosity can easily be defined, either by defining the grey values represent pore and grain, and measuring the average grey value in a suitably defined sub-volume. However the preferred technique for the low-pressure tests where grains do not break, is to define a threshold greyscale value, above which voxels are considered to be grain and below which they are considered to be pore – the value is chosen to obtain the solid volume of grains measured by weighing at the end of the test. Porosity is then easy to define in a sub-volume in such an image: the volume of voids and solids are simply counted.

Binary images where the solid and void phases are defined are the starting point for the definition of individual grains: the solid phase is split into individual grains using a watershed as described in Andò et al. (2012a). Each grain (i.e., all the voxels making up an individual grain) is then given a unique number, and properties of these 3D sets of voxels (position, volume) can be measured. The splitting and labelling procedure is repeated for each imaged state, and since grains will not have the same unique number, labels are reconciled by tracking grains from increment to increment using a specifically developed technique called ID-Track (Andò et al., 2012a). Following the change in the centre-of-mass of each grain over an increment gives a very precise evaluation of the displacement of the particle (with an error less than 0.1 pixels).

The measurement of rotations is more challenging: at this resolution the grain shapes are not detailed enough for the long and short axes of the moment of inertia tensor to be stable. To overcome this problem, a discrete DIC (digital image correlation) technique has been proposed in Andò et al. (2012b), where tracked grains are matched based on their images – this combined with ID-Track gives the full rigid body motion of the grains.

3. Results

The measurements that can be obtained with the combination of tools detailed above are shown, for an example test, in Figure 1. In the top of the figure, a schematic of the in-situ setup is shown, along with the macroscopic results obtained from the force and displacement measurements.

Figure 1 shows schematically the steps of image processing required to reconstruct a 3D image, and then to define and follow grains between imaged states, allowing measurement of their kinematics. The series of vertical slices presented at the bottom of the figure shows vertical slices taken through the specimen at points during the test, where all grains are coloured by their incremental rotations. Above these maps of discrete quantities, is a map of a continuum mechanics quantity of shear strain, measured on tetrahedra defined by tesselating grain centres.

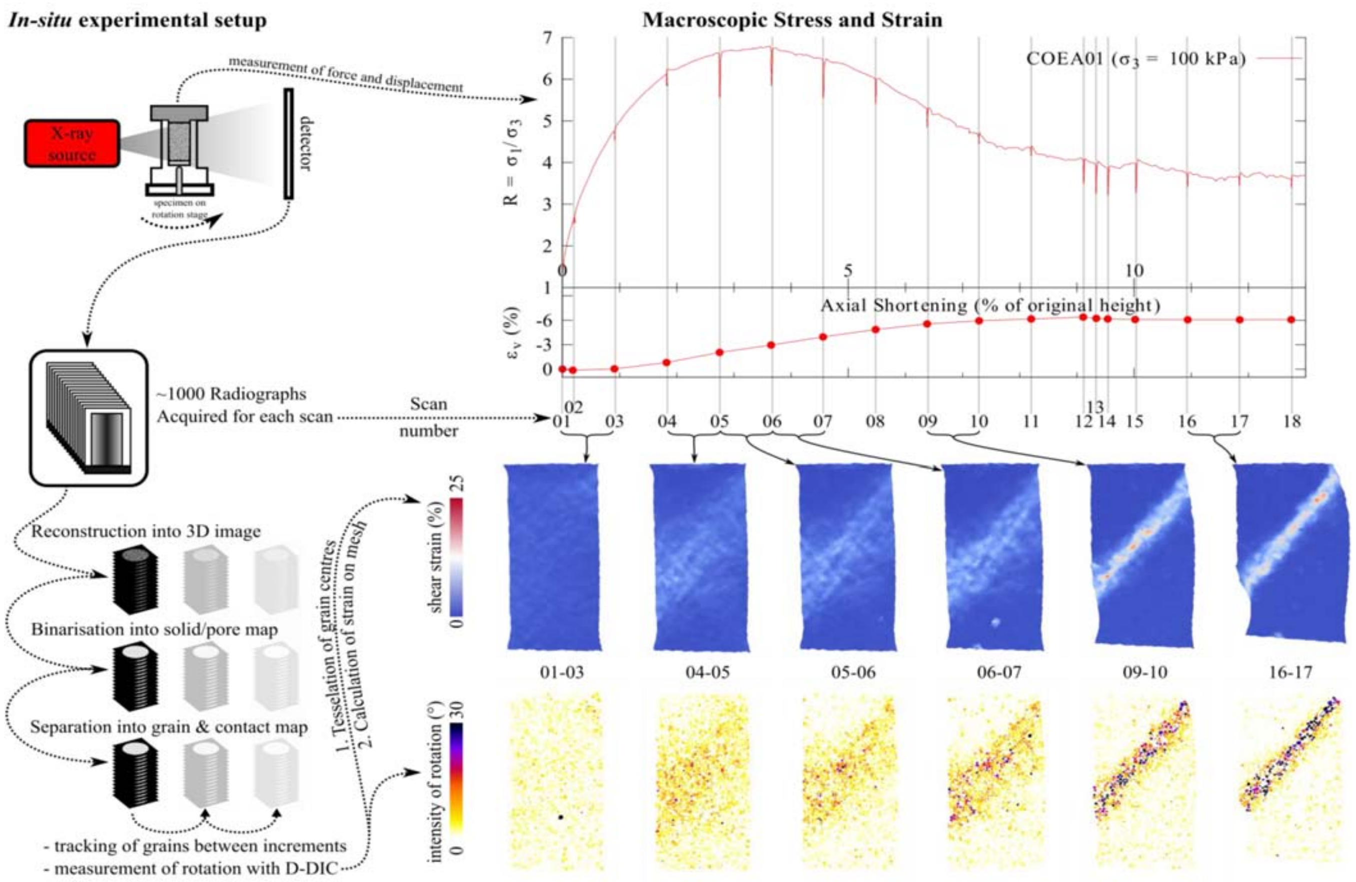

Figure 1. Illustration of the procedure for the analysis of in-situ experiments, with some highlighted results

It is clear that this kind of discrete 3D information available all the way through a mechanical test represents an experimental revolution in geomechanics – recent publications such as Desrues and Andò (2015) show how, for example, the residual state of stress in specimens with different angularities is easy to relate to the grain-scale kinematics at play in the shear band.

4. Challenges

Future work will focus on two areas: solving current measurement challenges for the subject presented above, as well as elucidating new phenomena using 3D images and data processing tools similar in spirit as those presented.

4.1 Current measurement challenges for grain kinematics

The rotations of grains, as well as the shear strain maps derived from grain displacements highlight some interesting phenomena. Especially before the macro-peak, there are some interesting chains of rotating grains that can even be seen in the vertical section shown (in 3D the chains are clear to see, but unfortunately analysing this structure in 3D as well as showing it in print also remains an open challenge). The emergence of a wide band of rotating grains that concentrates into a final shear band is also very interesting, and the grain-scale reasons for this collective behaviour are doubtlessly to be found in the way that forces are transmitted from grain to grain. Looking at the grain maps, we can see that a specimen with significantly fewer grains would not have had the degrees of granular freedom in order to exhibit such a shear band. Unfortunately, having sufficient resolution to study grain kinematics does not appear, using standard tools, to offer enough to study grain-to-grain contacts, as shown in Andò et al. (2013) and illustrated in Figure 2 – the number of voxels describing the contact between the two objects is simply insufficient. Problems appear both in the counting of contacts (they are systematically overestimated – see Wiebicke et al., 2015), as well as the extremely poor definition of their orientation.

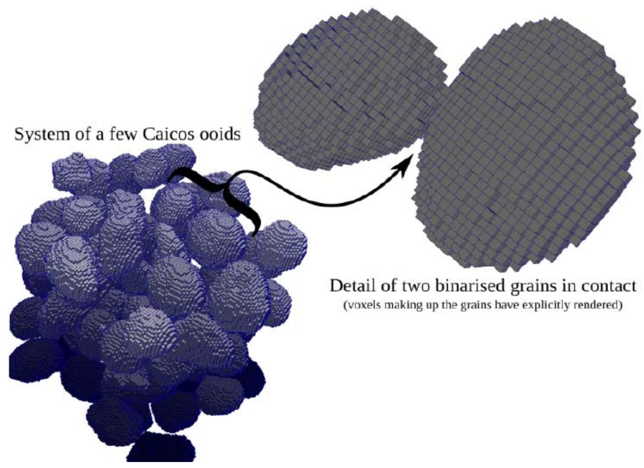

Figure 2. A collection of 31 Caicos ooids grains, shown with a zoom on two grains in contact

Some work in collaboration with discrete mathematicians has allowed this measurement to be made in some idealised cases using a Random Walker (see Viggiani et al., 2013, the base of this algorithm is now implemented in the python toolkit skimage – see Van Der Walt et al., 2014), and the application of this sort of tool is part of the ongoing PhD work of M. Wiebicke, with the objective of obtaining a fabric tensor from such measurements. Another approach to the scarcity of information is to use geometrical models to capture grain shapes, either in the style of level sets (see Andrade et al., 2012 and upcoming work), or in the style of spherical harmonics (see Zhao et al., 2015). Work on all fronts is extremely important to get further in the characterisation of the complex phenomenon of shear banding.

4.2 Highlighting any grain-scale phenomena with tomography

The ability to non-destructively image multiple states of a granular medium in 3D offers tremendous possibilities in the quantification of many phenomena in granular materials. In Grenoble, a number of different phenomena are being investigated at the time of writing. The three-phase interaction of soil-water-air mix with a focus on the water-retention behaviour of soil is an important area of focus (Kaddhour et al., 2013, with important work also done by other groups such as Sheel et al., 2008 and Higo et al., 2011. Kim et al., 2011 uses neutrons instead of x-rays to pick out the water), the study is currently being extended to the triaxial behaviour of partially saturated sand with a new triaxial setup. One of the main challenges here is the "trinarisation" of such a volume to distinguish all three phases without errors, this is a particular challenge in the case of water, since its density is low compared to sand grains.

Furthermore, the quantification of cement is also an important area of research work, be it "bio-cemented" materials such as those produced in U.C. Davis (DeJong et al., 2006) which have been studied with x-ray tomography (Tagliaferri et al., 2011), or artificially cemented material (see Das et al., 2013 as well as Tengattini et al., 2015). Challenges here include the difficult quantification of cement and its evolution between grains (since both can be of similar greyscale values).

One last major area of work is grain breakage (as illustrated in Figure 3), where the challenge is to quantify the process of breakage, even when particle shapes are evolving, and particle sizes are becoming small. When particles fall below the resolution of the measurement, only their average mass can be followed, and taking this into account in an algorithm is certainly a big challenge. Observations of breakage in triaxial compression (Alikarami et al., 2014) show that this is a rich field for exploration, and the ongoing PhD thesis of Z. Karatza is in this direction. Results of compression tests on a few particles (Cil and Alshibli, 2012) also highlight some interesting particle-level mechanisms.

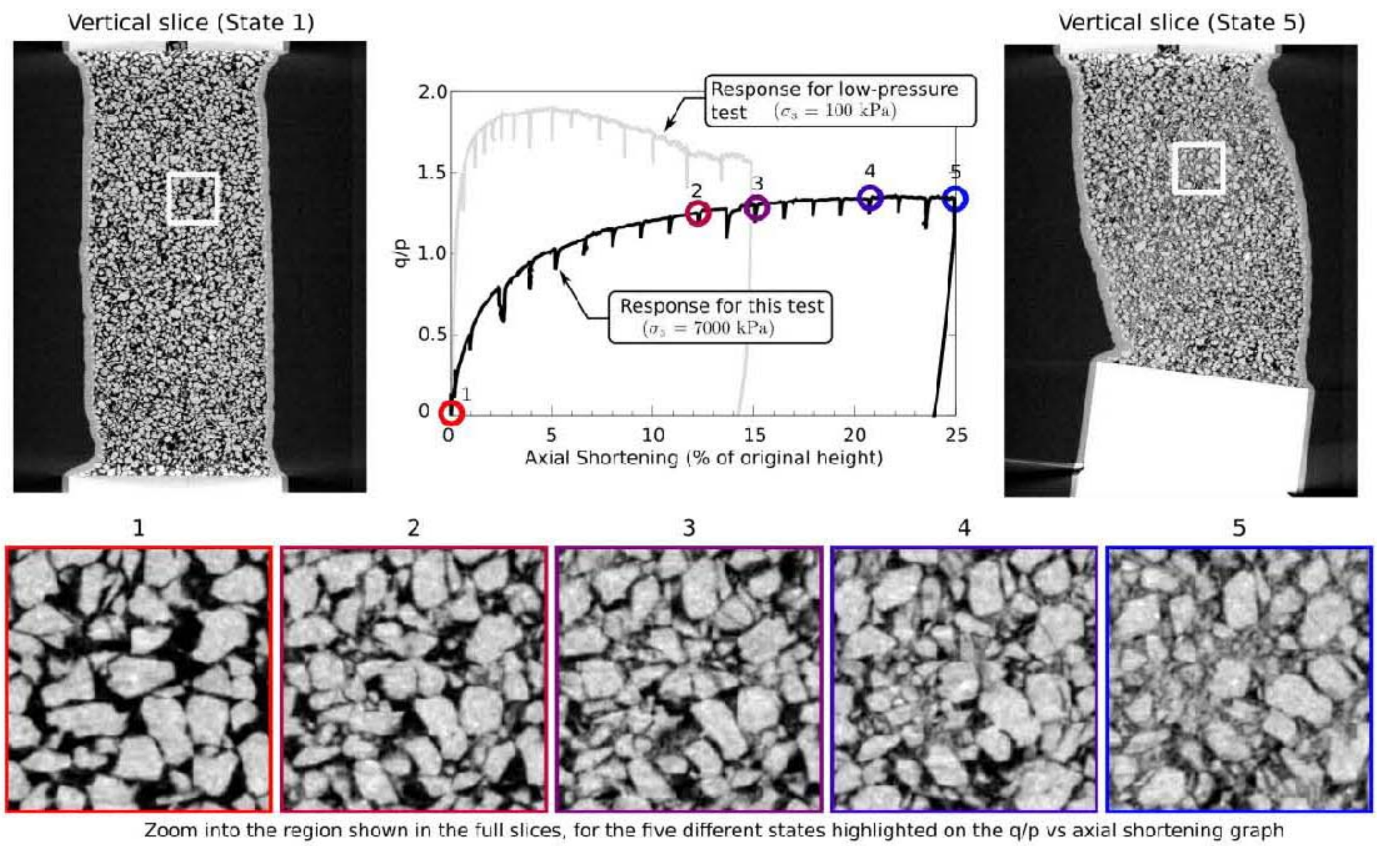

Figure 3. Some observations of grain breakage from Andò et al., 2013

5. Conclusions

X-ray tomography, and its application to geomaterials is becoming a very powerful tool in this field. The ability to acquire images with a resolution of tens of microns allows the grain-scale to be accessed in sand, and phenomena to be characterised at this scale. This kind of measurement opens many doors: to treat particles discretely and analyse their collective behaviour with complex networks (see Tordesillas et al., 2015), as well as discrete particle-by-particle simulations (Andrade et al., 2012). Many open measurement questions remain, since the development of accurate and well-characterised image analysis tools require careful procedures, however the tempting prospect of answering long-standing macro-questions at the micro-scale makes the challenge worth facing.

Acknowledgements

Laboratoire 3SR is part of the LabEx Tec 21 (Investissements d'Avenir - grant agreement n°ANR-11-LABX-0030).

References

Alikarami, R., Andò, E., Gkiousas-Kapnisis, M., Torabi, A., & Viggiani, G. (2014). "Strain localisation and grain breakage in sand under shearing at high mean stress: insights from in situ X-ray tomography", *Acta Geotechnica*, 10(1), 15-30.

Alshibli, K. A., & Hasan, A. (2008). Spatial variation of void ratio and shear band thickness in sand using X-ray computed tomography. *Geotechnique*, 58(4), 249-257.

Andò, E., Hall, S. A., Viggiani, G., Desrues, J., and Bésuelle, P. (2012a), "Grain-scale experimental investigation of localised deformation in sand: a discrete particle tracking approach", *Acta Geotechnica*, Vol. 7, No. 1, pp. 1–13.

Andò, E., Hall, S. A., Viggiani, G., Desrues, J., and Bésuelle, P. (2012b), "Experimental micromechanics: grain-scale observation of sand deformation", *Géotechnique Letters*, Vol. 2, No. 3, pp. 107–112.

Andò, E., Viggiani, G., Hall, S. A., & Desrues, J. (2013). "Experimental micro-mechanics of granular media studied by X-ray tomography: recent results and challenges", *Géotechnique Letters*, 3, 142-146.

Andrade, J. E., Vlahinić, I., Lim, K. W., & Jerves, A. (2012). Multiscale 'tomography-to-simulation'framework for granular matter: the road ahead. *Géotechnique Letters*, 2 (July-September), 135-139.

Cil, M. B., and K. A. Alshibli (2012). "3D assessment of fracture of sand particles using discrete element method", *Geotechnique Letters*, 2: 161-166.

Das, A., Tengattini, A., Nguyen, G., & Einav, I. (2013). "A micromechanics based model for cemented granular materials", *Constitutive Modeling of Geomaterials* (pp. 527-534). Springer Berlin Heidelberg.

DeJong, J. T., Fritzges, M. B., & Nüsslein, K. (2006). "Microbially induced cementation to control sand response to undrained shear", *Journal of Geotechnical and Geoenvironmental Engineering*, *ASCE,* 132(11), 1381-1392.

Desrues, J., & Andò, E. (2015). Strain localisation in granular media. *Comptes Rendus Physique*, 16(1), 26-36.

Higo, Y., Oka, F., Kimoto, S., Sanagawa, T., & Matsushima, Y. (2011). "Study of strain localization and microstructural changes in partially saturated sand during triaxial tests using microfocus X-ray CT", *Soils and foundations*, 51(1), 95-111.

Kaddhour, G., Andò, E., Salager, S., Bésuelle, P., Viggiani, C., Hall, S., & Desrues, J. (2013). "Application of X-ray Tomography to the Characterisation of Grain-Scale Mechanisms in Sand". *Multiphysical Testing of Soils and Shales* (pp. 195-200). Springer Berlin Heidelberg.

Kim, F. H., Penumadu, D., & Hussey, D. S. (2011). "Water distribution variation in partially saturated granular materials using neutron imaging", *Journal of Geotechnical and Geoenvironmental Engineering, ASCE*.

Saadatfar, M., Francois, N., Arad, A., Madadi, M., Sheppard, A., Senden, T., & Knackstedt, M. (2013). "Grain-based characterisation and acoustic wave propagation in a sand packing subject to triaxial compression", *AIP Conference Proceedings* 1542 (pp 571-574).

Scheel, M., Seemann, R., Brinkmann, M., Di Michiel, M., Sheppard, A., Breidenbach, B., & Herminghaus, S. (2008). "Morphological clues to wet granular pile stability", *Nature Materials*, 7(3), 189-193.

Tagliaferri, F., Waller, J., Andò, E., Hall, S. A., Viggiani, G., Bésuelle, P., & DeJong, J. T. (2011). "Observing strain localisation processes in bio-cemented sand using x-ray imaging", *Granular Matter*, 13(3), 247-250.

Tengattini, A., Andò, E., Nguyen, G. D., Viggiani, G., & Einav, I. (2015). Double-scale assessment of micromechanics based constitutive models for granular materials undergoing mechanical degradation. *In Bifurcation and Degradation of Geomaterials in the New Millennium* (pp. 175-180). Springer International Publishing.

Tordesillas, A., Pucilowski, S., Tobin, S., Kuhn, M. R., Andò, E., Viggiani, G., ... & Alshibli, K. (2015). "Shear bands as bottlenecks in force transmission", *Europhysics Letters*, 110 (5), 58005.

Van der Walt, S., Schönberger, J.L., Nunez-Iglesias, J., Boulogne, F., Warner, J.D., Yager, N., Gouillart, E., Yu, T. and the scikit-image contributors (2014) "scikit-image: Image processing in Python", *PeerJ 2:e453.*

Viggiani, G., Andò, E., Jaquet, C., & Talbot, H. (2013). Identifying and following particle-to-particle contacts in real granular media: An experimental challenge. In POWDERS AND GRAINS 2013: *Proceedings of the 7th International Conference on Micromechanics of Granular Media* (Vol. 1542, No. 1, pp. 60-65). AIP Publishing.

Wiebicke, M., Andò, E., Herle, I., Viggiani, G. (2015) "Accurately measuring fabric and its evolution in sand", accepted abstract for *IS-Buenos Aires*, 2015.

Zhou, B., Wang, J., & Zhao, B. (2015). "Micromorphology characterization and reconstruction of sand particles using micro X-ray tomography and spherical harmonics", *Engineering Geology*, 184, 126-137.

Young Members' Arena, ISSMGE Bulletin: Volume 9, Issue 5, pp. 27-33

About the Young Member

Dr. Edward Andò is a young researcher applying in-situ x-ray tomography to the study of soil mechanics with the hope of elucidating the grain-scale mechanisms responsible for macroscopic behavior. He defended his PhD -- supervised by Jacques Desrues, Gioacchino (Cino) Viggiani and Stephen Hall -- in 2013 on this subject in Laboratoire 3SR, Grenoble and has stayed on in Laboratoire 3SR as a CNRS Research Engineer. The data coming from Dr. Andò's work has been studied and shared with a number of groups including most notably Jose Andrade's in Caltech and Antoinette Tordesillas' in Melbourne University. Current projects continue in this vein, trying to extract a fabric tensor from existing granular experiments, as well as applying x-ray tomography to the study of particle breakage, to three-phase problems (unsaturated soil mechanics), as well as more exotic problems such as fibre-reinforced soil.

Edward Andò, Gioacchino Viggiani, **Jacques Desrues**

a) Univ. Grenoble Alpes, 3SR, F-38000 (Grenoble, France),
b) CNRS, 3SR, F-38000 (Grenoble, France)

email: edward.ando@3sr-grenoble.fr
email: cino.viggiani@3sr-grenoble.fr
email: jacques.desrues@3sr-grenoble.fr

Hydrogeologists and Geotechnical Engineers – Lost Without Translation

Philip Pells and Steven Pells, Pells Consulting and University of New South Wales

ABSTRACT

Fundamental to structural, geotechnical, hydraulic and groundwater engineering are coherent, functional, mathematical theories that obey the laws of physics and thermodynamics. Whether explicit, or intuitive, and though they be simplifications of a complex reality, it is these theories that set engineers apart from lay persons.

Like all practitioners, hydrogeologists have developed categorisations of common phenomena to make their tasks easier, of which two that are ubiquitous in hydrology are:

1. The notion of 'aquifers', and their inverse; 'aquicludes' and 'aquitards'
2. The notion of 'confinement', and its inverse; 'connectivity'.

These relate to geology, and mathematics, and are enticing because geology is complex and mathematics can be difficult. While the categorisations have been helpful, where the only consideration is groundwater production, they are deceptions when it comes to assessing depressurisation impacts. In addition they are not scientifically quantifiable with satisfactory precision.

The categorisations form a heuristic, where:

"heuristics are simplified rules of thumb that make things simple and easy to implement. Their main advantage is that the user knows they are not perfect, just expedient, and is therefore less fooled by their powers. They become dangerous when we forget that." (Taleb, 2012)

In this paper, we trace the etymology of the classification of 'aquifers' and 'confinement', and the development of the current hydrogeologist's heuristic. We show how this leads to a contagion of error when considering depressurisation impacts. We also deal with other words and concepts that are particular to hydrogeology, being Specific Storage, Hydraulic Diffusivity, Specific Yield, Specific Retention and Transmissivity, and which often mystify civil engineers with conventional training in soil mechanics. By translating these hydrogeology terms to those understood by engineers we hope to help communications between these closely aligned professionals.

1. INTRODUCTION

Hydrogeologists and geotechnical engineers typically reach their professions by different academic routes – the former mostly from geology and the latter mostly from civil engineering. For historical reasons these disciplines have adopted substantially different words to express and define what are identical physical and mathematical facts and concepts. The net result is that much of the time professionals of the one kind don't know what the other kind are talking about.

In addition these professions have adopted different heuristics to make their tasks easier, heuristics being:

"…*simplified rules of thumb that make things simple and easy to implement. Their main advantage is that the user knows they are not perfect, just expedient, and is therefore less fooled by their powers. They become dangerous when we forget that".* (Taleb, 2012)

Thus geotechnical engineering is based substantially on the theory of linear elasticity, even though real geotechnical materials are neither elastic, nor linear. Hydrogeologists in turn depend substantially on two heuristic classifications, these being the notions of:

- 'aquifers', and their opposites; 'aquicludes' and 'aquitards', and
- 'confinement' and its inverse 'connectivity'.

It is the purpose of this paper to connect the languages of hydrogeology and geotechnical engineering, and also to demonstrate that the heuristics adopted, can have important negative consequences. This accords with the point made by Daniel Kahneman:

"This is the essence of intuitive heuristics; when faced with a difficult question, we often answer an easier one instead, usually without noticing the substitution."

We deal with words and concepts that are particular to hydrogeology, being Specific Storage, Hydraulic Diffusivity, Specific Yield, Specific Retention and Transmissivity, and which often mystify civil engineers with conventional training in soil mechanics. By translating these hydrogeology terms to those understood by engineers we hope to help communications between these closely aligned professionals.

We also trace the etymology of the classification of 'aquifers' and 'confinement', and the development of the current hydrogeologist's heuristics, and suggest that, in some situations, these heuristics are misleading, and no longer necessary.

2. MATHEMATICAL FUNDAMENTALS THAT ALLOW THE TRANSLATIONS

Boussinesq (1877 and 1902) established the mathematics of transient groundwater flow through porous media by combining the differential equation of flow with the equation of continuity. The resulting equation is the same as the heat equation determined by Fourier (1807, 1822) – see Figure 1. The only difference is that gravity plays a role in groundwater flow.

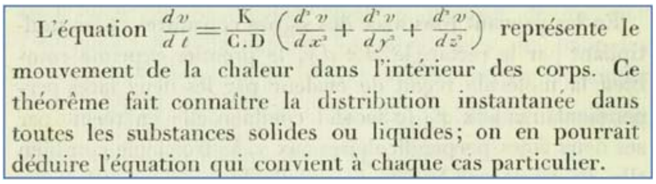
L'équation $\frac{d^2v}{dt} = \frac{K}{C.D}\left(\frac{d^2v}{dx^2}+\frac{d^2v}{dy^2}+\frac{d^2v}{dz^2}\right)$ représente le mouvement de la chaleur dans l'intérieur des corps. Ce théorême fait connaître la distribution instantanée dans toutes les substances solides ou liquides; on en pourrait déduire l'équation qui convient à chaque cas particulier.

Figure 1. The heat equation as published by Fourier (1822)

There are about as many versions of the transient groundwater flow equation as there are publications on the topic, with authors choosing to use different symbols and words for the same thing[1]. We consider that a neat presentation of the relevant equations are by Biot (1941).

The equation for flow in three dimensions is:

$$\nabla h^2 = \frac{1}{c}\frac{\partial h}{\partial t} \qquad (1)$$

where h = potentiometric (hydraulic) head = $(p/\gamma_w)+z$; t = time, (T); ∇ = Laplace operator; c = consolidation coefficient (L^2/T).

[1] For example, in a simple matter, it is found that the parameters for permeability and hydraulic conductivity are termed, and symbolised as:

K *'Intrinsic Permeability'* L^2 (Verruijt 1970)
K_i *'Permeability'* L^2 (Kresic 2007)
k *'Coefficient of Permeability'* L/T (Verruijt 1970 and Biot 1941)
K *'Hydraulic conductivity'* L/T (Kresic 2007)

If there is full saturation the consolidation coefficient is:

$$c = \frac{k}{\alpha \gamma_w} \quad (L^2/T) \tag{2}$$

where k = hydraulic conductivity (L/T); γ_w = unit weight of water (M/L^2T^2); α = compressibility of the bulk ground (LT^2/M), which is equal to

$$\frac{(1+\nu)(1-2\nu)}{E(1-\nu)} \tag{3}$$

where ν =Poisson's ratio; E =Young's Modulus (M/LT^2).

Equations 1 to 3 are for any transient flow problem in a saturated compressible medium. They assume Darcy seepage, small strain theory, linear elasticity and permeability independent of effective stress. They also assume that water is incompressible, although compressibility of the pore fluid requires only a minor modification to Equation 1.

These assumptions are reasonable for most civil engineering applications including assessing macro-seepage through fractured rock masses. The equations can be generalised for anisotropy and for partly-saturated conditions. Equation 1 allows one to perform key translations.

Firstly, Biot's Consolidation Coefficient is:

- identical to **Hydraulic Diffusivity** as used in the hydrogeology literature,
- equivalent to Thermal Diffusivity in the heat equation, and
- the same as Terzaghi's Coefficient of Consolidation.

Hydrogeologists use three other terms in association with Equation 1. They and their translations are:

- **Specific Storage** (also called **Specific Storativity**) - being the product of compressibility and unit weight of water, viz:

$$S_s = \alpha \gamma_w \; (1/L) \tag{4}$$

- **Storage Coefficient** (also called **Aquifer Storativity** or **Storativity**) – being the product of **Specific Storage** and the thickness of a defined 'aquifer' (b), viz:

$$S = S_s b \;\; \text{(unitless)} \tag{5}$$

As a word of caution it must be noted that at depths dealt with in reservoir engineering for the oil industry, compressibility of pore fluids becomes significant, with the result that the equations for Specific Storage and Storativity are different to those given above, but which are applicable to most civil and mining engineering projects.

Hydrogeologists also make much use of the term 'transmissivity', which is simply Hydraulic Conductivity multiplied by the thickness of a defined 'aquifer': T = kb.

A particular case has to be addressed where there is a phreatic surface[2] in the groundwater regime under consideration. When the phreatic surface changes water either drains from the ground above the surface as the surface lowers, or water may go into storage as the surface rises. This is the situation hydrogeologists refer to as an **Unconfined Aquifer**. Computations in this situation require modifications to Equation 1, requiring a measure of what Meinzer (1932) called **Effective Porosity**[3] and which most hydrogeologists call the **Specific Yield**[4]. In soil mechanics terminology this parameter has been called **Specific Porosity**[5].

3. DERIVATION OF PARAMETERS

Given the above translations it can be seen that, for the assumption of linear behaviour, it is only necessary to determine five parameters for each material type, namely:

- Mass Young's modulus of a jointed rock mass, or the mass Young's modulus of the soils in question[6]
- Mass Poisson's ratio
- Effective porosity
- Hydraulic conductivity

Geotechnical engineers can usually make reasonable assessments of the likely range of Young's Modulus values; and Poisson's ratio (which is usually between 0.15 and 0.4). Effective Porosity can also be assessed within reasonable ranges, being close to true porosity for gravel, and almost zero for clays and mudstones. However, in-situ permeability values, and anisotropy of permeability, are usually only known to orders of magnitude. In the example given above, this uncertainty changes a benign 200 years to an unacceptable 20 years.

In the near horizontally bedded Triassic strata of the Sydney Basin, which have been investigated for very many underground mining and civil engineering projects, there are very wide ranges of measured hydraulic conductivity values, and even wider ranges adopted by analysts (see Figure 2). It can be seen that there are differences of up to 3 orders of magnitude in respect to adopted permeability values. It can also be seen that, for the Bald Hill Claystone, there is no correlation between the field tests and adopted parameters.

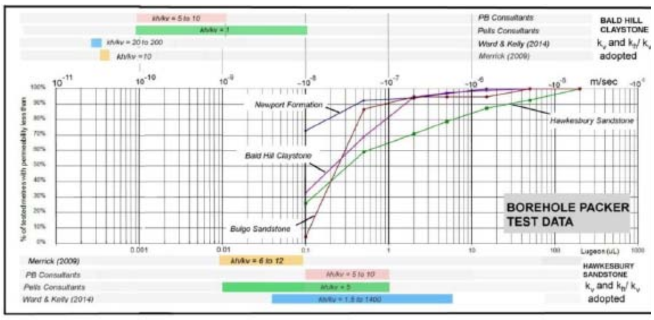

Figure 2. Differences in hydraulic conductivity parameters adopted in the Sydney Basin compared with laboratory tests

In addition there is the observation that permeability values decrease with depth in each stratigraphic unit (Tammetta and Hawkes, 2009).

Therefore, it is obvious that uncertainties in hydraulic conductivity values dominate computations of groundwater flow quantities and depressurisation, these being independent factors. Sensitivities to compressibility and volumetric water content is secondary.

It has already been noted that the above parameters are for assumed linear behaviour. With the power of modern numerical analyses one is not limited to the linear assumption and usually assessments have to be made of:

---

[2] The phreatic surface is at atmospheric pressure; some distance above the surface where pore pressures are negative, air is sucked into the voids causing partial saturation. This is a highly non-linear situation where hydraulic conductivity changes and high matric suctions are generated.

[3] "volume of interconnected pore space that allows free gravity flow of groundwater" (Kresic 2007).

[4] "that volume of water in the pore space that can freely drain due to change in the hydraulic head" (Kresic 2007).

[5] Bishop (1967).

[6] Measured from strains under change of effective stress.

- Hydraulic conductivity versus pore pressure (for negative pore pressures).
- Volumetric water content versus pore pressure.

The first of these two functions is very difficult to know and should be studied by parametric variation for a particular analysis. Such parametric investigations are essential for a particular project to obtain an understanding of the impacts of the engineering heuristic of linear behaviour.

4. THE HEURISTICS OF HYDROGEOLOGY

4.1 The Key Problem

A key problem in hydrogeology was that for about 180 years Equation 1 could not be solved for most real situations. So, using Kahneman's language, *"when faced with a difficult question, we often answer an easier one instead...".*

This difficulty went hand in hand with the earliest work in hydrogeology which was concerned with understanding the artesian groundwater resources of France and Italy.

4.2 Development of Understanding of Artesian Groundwater

The word *'aquiféres'*, meaning liquid bearing, was used by the French Zoologist, Lamarck (1830), in describing vessels of the lungs, some being air-bearing (*trachées aèriféres)* and some carrying blood (*trachées aquiféres).*

The same word, *aquiféres*, was then used in 1835 by Lamarck's colleague, Francois Arago. Writing in the *Annuaire Le Bureau des Longitudes (p225*), in regard to artesian bores and springs, he said:

*"Let's remember now the way rain waters penetrate some stratified land layers; let's keep in mind that it's only on the hill slopes or at their crest that the section of the layers is exposed; that this is their water intake; so it always occurs at height. Let's think, in addition, that these **aquifer** layers, after going down along the slope of the hills that broke them a long time ago by raising them, extend horizontally or almost horizontally across the plains and that they are often sort of enclosed between two impermeable layers of clay or rock. So we will conceive the existence of underground **aquifers** that are, naturally, in the same hydrostatic conditions as the commonplace ducts, whose soutérazi give us a model. And that a borehole drilled in the valleys, through the upper ground down to and including the highest of both waterproof layers, within which the **aquifer** is enclosed, will become the second branch of the U-shaped pipe we mentioned at the beginning of this chapter, or if you like of an inverted water trap, or, even better, of a soutérazi. The fluid will rise inside this borehole, to the height the corresponding **aquifer** attains on the hillsides it originated from.*

*From there, everyone should understand how, on a given horizontal ground, underground waters, placed at different levels, can have different upwards forces; from there, everyone will explain why the same **aquifer** rushes here at great heights, while it fails to reach ground level further. Simple level inequalities will become the sufficient cause, the natural cause of all these inconsistencies."*

By way of explanation, the word *soutérazi* relates to the square obelisks, or pillars, erected in valleys between the supply reservoir and the city of Constantinople (see Figure 3), such that "*the level of the top of every successive pillar varies analogous to an inclined plan commencing at the mountains*" (Matthew, 1835).

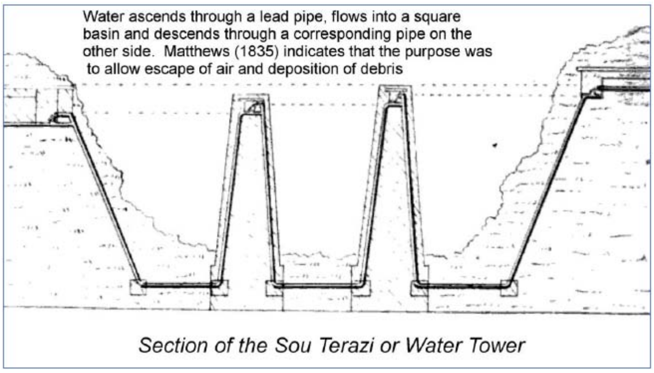

Figure 3. Soutérazi along the water supply to Constantinople

It is clear from Arago's work that he intended the word *aquifer* to have a similar connotation to *aqueduct*, and to imply the characteristics of a conduit. The purpose was to explain artesian springs, a matter which at that time was somewhat controversial. The concept allowed linkage to the known science of hydrostatics (Pascal, 1647), and the conveyance of city water supplies as described by Darcy (1856) and Matthews (1835).

In 1836, the Rev William Buckland, who was familiar with Arago's work, produced a cross-section showing the genesis of artesian wells beneath London (see Figure 4). He did not use the word *aquifer*.

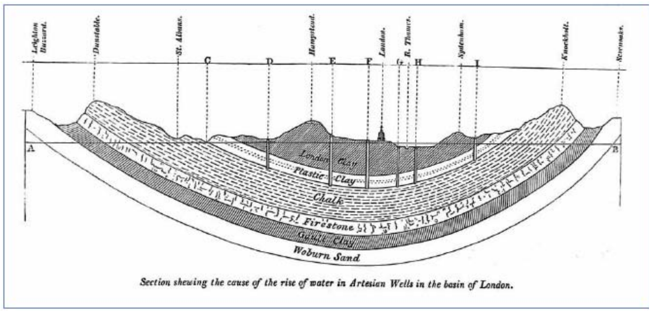

Figure 4. The artesian wells of London, William Buckland, 1836

We do not know when the terms *aquitard and aquiclude* were first used. They do not appear in the works of Meisner (1923 and 1928), but what became important is that he encapsulated the essence of these words in the concept of *'confinement'* of an aquifer. Thus in 1923 he wrote:

*"... **serves to confine** the water of the Lissie gravel under artesian pressure"* (Meissner, 1923, p 308)

In 1928 he presented this idea diagrammatically as reproduced in Figure 5.

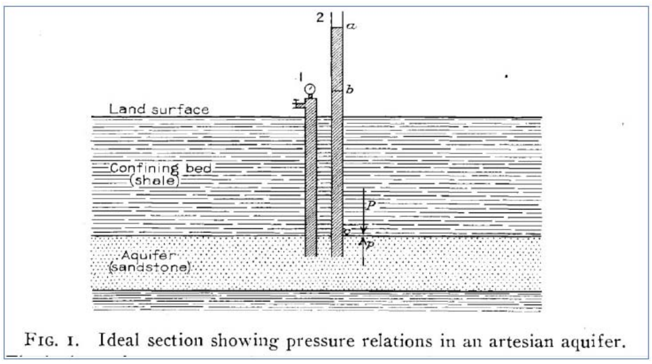

Figure 5. Confined aquifer, Meisner, 1928

In the real world, the differentiation between aquicludes, aquitards and aquifers is unclear. There is no accepted standard of measurement which differentiates or defines them in relation to geological formations which are a continuum of materials with wide ranging properties in regard to how water is stored and transmitted. There is also no accepted standard of measurement which differentiates or defines whether a portion of ground is 'confined' or 'unconfined'.

This confusion was unacceptable to C V Theis, who, 52 years after his famous paper on transient flow to wells (Theis, 1935), and shortly before his death, dictated the last changes to a paper titled, "Aquifers, Ground-Water Bodies and Hydrophers". In this he said:

"Thus, "aquifer" has been used in so many different senses by so many people to express their own particular ideas that it has become an Alice-in-Wonderland word that means just what the author says it means. Worst of all, the author practically never tells us what he means. It has been used in so many different ways that it must be abandoned entirely as a scientific word or alternately to express only the original usage of it without any relation to the water table ….." (Theis, 1987)

4.3 The Co-Development of Approximate Solutions to the Diffusion Equation

The first mathematical heuristic applied to solving the diffusion equation for groundwater (Equation 1) was by Dupuit (1863) who postulated that groundwater flows horizontally in an unconfined aquifer, and that the groundwater discharge is proportional to the saturated aquifer thickness[7]. The essence of the assumptions is that equipotentials are vertical.

From this, Dupuit derived an approximate equation for flow to a well, namely:

$$Q = \pi k \frac{(H^2 - h_0^2)}{\log(L/R)} \qquad (6)$$

where the terms are shown in Figure 6, and L is "*le rayon du massif filtrant"*.

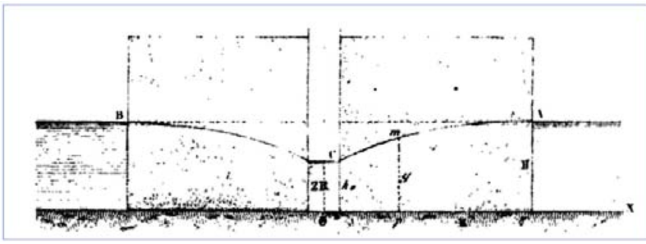

Figure 6. Dupuit (1863) Figure 65; analysis of flow to a well in a sand island

Obviously the error arising out of the Dupuit assumption relates directly to the degree to which the actual flow pattern diverges from horizontal, meaning equipotentials are not vertical.

Thiem (1870) made the equation useful by showing that beyond a certain distance from a well, drawdown of the potentiometric surface becomes negligible, and Theis (1935) extended the solution to non-steady state in a, so-called, confined aquifer.

All of these reinforced the heuristic of horizontal flow, and reinforced the use of aquifers, aquicludes and transmissivity.

[7] Dupuit actually addressed flow to a well within a circular island of sand.

The impact of Dupuit's heuristic grew to the point where now, the most widely used 3D groundwater software, MODFLOW, was created within the framework of that heuristic.

There is no doubt that the Dupuit assumption was, and is, valuable where the prime purpose is furnishing a supply of groundwater. But the simplifications have locked in obeisance to horizontal flow and have fed poor understanding of groundwater depressurisation. The fundamental difference between flow quantity, and depressurisation has become lost. Depressurisation and drawdown became synonyms, which they are not.

Depressurisation, involves changing the shapes of equipotentials; typically changing them from near vertical to near horizontal.

5. DISCUSSION

We consider that the lexical differences that have developed between hydrogeologists and geotechnical engineers for what are exactly the same concepts and parameters is an accident of history arising from a combination of the early studies of artesian groundwater systems, and inability to solve the diffusion equation without invoking grossly simplified boundary conditions.

We consider that modern computational methods render many of the historical terms, and analytical methods obsolete, and have led to a contagion of error when considering depressurisation impacts of tunnels, deep basements, open pit mines and underground mines. These impacts can be assessed, not precisely, but within reason, by disregarding the heuristic of horizontal flow, and by heeding the advice of Theis (1987) to the effect that the use of the word aquifer "*should be abandoned entirely as a scientific word or alternately to express only the original usage".*

References

Arago, F. 1835, Sur les Puits Forés, Connus Sous Le Nom de Puits Artésiennes, De Fontaines Artésiennes, Ou de Fontaines Jaillissantes. Notices Scientifiques; Le Bureau des Longitudes, Paris.

Bergles, A. E. 1988, History of Heat Transfer, Essays in Honour of the 50th Anniversary of the ASME Heat Transfer Division. The American Society of Mechanical Engineers.

Biot, M. A. 1941, General Theory of Three-Dimensional Consolidation. Journal of Applied Physics, Vol 12, No. 2 pp 155-164, Feb.

Brown, G. V. 2004, Jules Dupuit's Contributions in Water Resource. Water Resources and Environmental History, ASCE.

Buckland, W. 1836, Geology and Mineralogy considered with reference to Natural Theology. London, William Pickering.

Darcy, H. 1856, The Public Fountains of the City of Dijon. English translation, Patricia Bobeck, Kendall Hunt Publishing 2004.

De Wiest, R. J. M. 1965, History of the Dupuit – Forcheimer Assumptions on Groundwater Hydraulics. Transactions ASAE.

Dupuit, J. 1863, Estudes Thèoriques et Pratiques sur le mouvement des Eaux dans les canaux dècouverts et à travers les terrains permèables (Second Edition ed.). Paris: Dunod.

Howden, N and Mather, J (Editors) 2013, History of Hydrogeology. CRC Press.

Independent Expert Scientific Committee, Department of Environment, Australia, June 2014, www.iesc.environment.gov.au.

Kahneman, D. 2011, Thinking Fast and Slow, Allen Lane.

Kresic, N. 2007 Hydrogeology and Groundwater Modelling, 2nd Ed CRC Press, Taylor & Francis Group.

Lamarck, J. B. P. A. 1830, Philosophie Zoologique ou Exposition. Germer Baillére Library, Paris, 1830.

Matthew, W. 1835, Hydraulia, an Historical and Descriptive Account of the Water Works of London. Simpkin, Marshall & Co, London.

Meinzer, O. E. 1923, The occurrence of ground water in the United States, with a discussion of principles. U.S. Geological Survey Water-Supply Paper 489. 321 p.

Meinzer, O. E. 1928, Compression and elasticity of artesian aquifers. Journal of Economic Geology, 23 (3), 263-291.

Norton, W. H. 1897, Artesian wells of Iowa. Iowa Geological Survey, 6, 113-428.

NSW Department of Planning. 2008, Southern Coalfields Enquiry, Impacts of Underground Coal Mining on Natural Features in the Southern Coalfield. Strategic Review. July 2008.

Pascal, B. 1647, Recit de la Grande Experience de l'Equilibre des Liqueurs. Paris.

Taleb, N. N. 2007, The Black Swan, Random House, New York.

(ISSMGE Bulletin: Volume 9, Issue 6 Page 42, pp. 42-50)

ΕΛΛΗΝΙΚΕΣ ΤΕΧΝΟΛΟΓΙΚΕΣ ΕΞΕΛΙΞΕΙΣ ΣΤΗΝ ΓΕΩΜΗΧΑΝΙΚΗ κ.α.

Ενόργανη Παρακολούθηση Παραμορφώσεων με Αισθητήρες Οπτικών Ινών

Αρχές δομικής παρακολούθησης

Η παρακολούθηση της δομικής ακεραιότητας των κατασκευών (Structural Health Monitoring) αποτελεί ένα νέο επιστημονικό πεδίο, που έχει σκοπό να παράσχει κατά το δυνατόν αξιόπιστα στοιχεία σχετικά με την κατάσταση του φορέα υπό παρακολούθηση (ύπαρξη ατελειών, αστοχιών, φορτίσεις, εντατική κατάσταση κλπ), προκειμένου να αποφασισθεί η ενδεχόμενη αποκατάστασή του με τον πλέον κατάλληλο τρόπο. Γενικά, αποτελεί μία προσπάθεια επίλυσης αντίστροφου προβλήματος.

Τα κύρια βήματα, τα οποία περιλαμβάνει η **μεθοδολογία της δομικής παρακολούθησης** είναι συνοπτικά τα ακόλουθα:

- Επιλογή των θέσεων για την ανάπτυξη του δικτύου αισθητήρων.
- Προσδιορισμός του τύπου των αισθητήρων που θα χρησιμοποιηθούν, ανάλογα με το είδος των μετρούμενων μεγεθών, την απαιτούμενη ακρίβεια και το περιβάλλον λειτουργίας. Η καλύτερη διαθέσιμη μορφή σύνθετου αισθητήρα παρέχει τη δυνατότητα περιγραφής της ελαστικής γραμμής του φορέα, ενώ ταυτόχρονα, σύμφωνα την αρχή της αναστρεψιμότητας των επεμβάσεων σε μνημεία, επιτρέπει την τοποθέτηση και άρση του κατά βούληση.
- Λήψη μετρήσεων από τους αισθητήρες.
- Σύγκριση των μετρήσεων που ελήφθησαν από τους αισθητήρες ως προς την πρότυπη συμπεριφορά της κατασκευής.
- Θέσπιση ορίων συναγερμού

Τεχνικά χαρακτηριστικά οπτικών αισθητήρων - Φυσική αρχή λειτουργίας

Διακριτική Ικανότητα	0.2 pm	**Μήκος Κύματος**
	0.2 μstain	**Παραμόρφωση**
	0.02 °C	**Θερμοκρασία**
Οπτικό Καλώδιο	Διάμετρος 3mm Προστασία PVC – Ίνες Κέβλαρ.	
Τύπος Οπτικής Ίνας	Μονότροπη 9/125μm - Ακρυλική επένδυση 250μm	
Τύπος Αισθητήρα	Μήκος Κύματος 1520 - 1570nm R>90%	
Μήκος Αισθητήρα	0.1–10mm	
Εύρος Μέτρησης	± 20,000 μstrain	
Οπτικός Σύνδεσμος	FC / APC	
Παροχή Ηλεκτρικής Ισχύος	-	
Θερμοκρασία Λειτουργίας	-100 °C έως 300 °C	

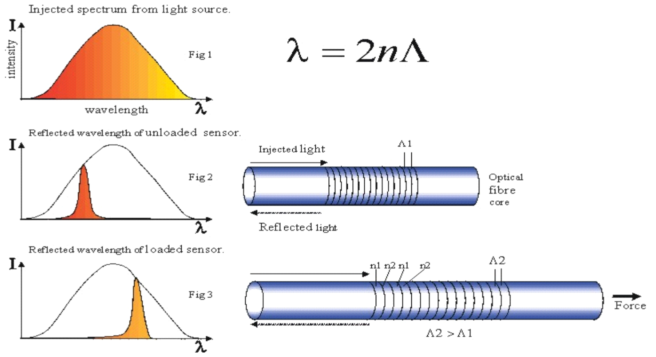

Παρακολούθηση της Δομικής Ακεραιότητας του Τείχους της Ακρόπολης

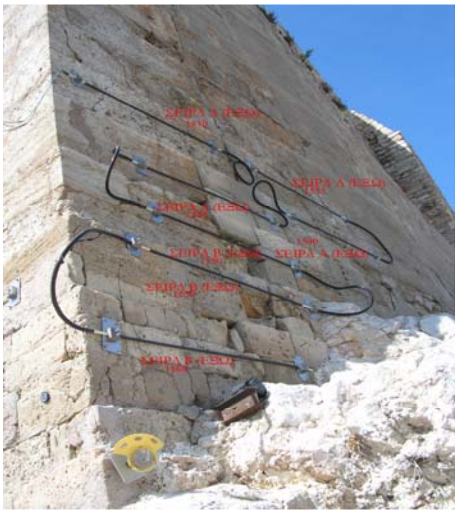

Instrumentation of the T3 & Γ9 Motorway Bridges of Egnatia Odos

T3 Motorway Bridge

The T3 bridge has three 28m long openings, each with seven prefabricated, prestressed beams. The T3 bridge is a typical bridge of the Egnatia motorway. Thus, its instrumentation provided great interest and was considered to be of utmost importance.

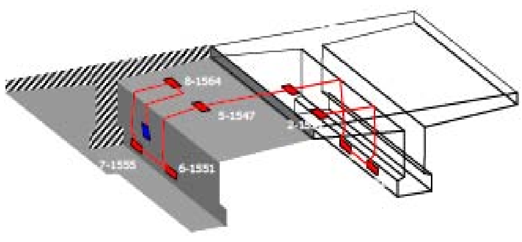

8 Fibre Bragg Grating optical sensors were installed on the beams bearing the largest load due to heavy vehicle traffic, as shown in the image above.

Γ9 Motorway Bridge

The Γ9 bridge was constructed with the balanced cantilever method. It has two 85m long post-tentioned concrete openings. The Γ9 bridge is also a typical bridge of the Egnatia motorway, thus being ideal for structural monitoring.

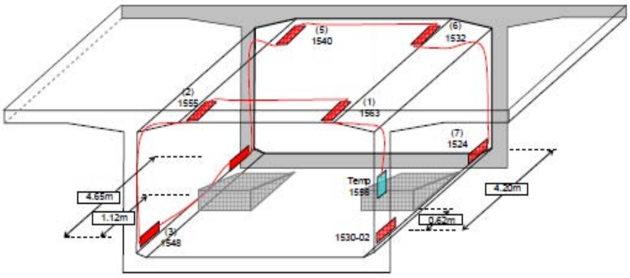

8 Fibre Bragg Grating optical sensors were installed on the elements most affected by creep after the cantilever's final placement.

The sensors were incorporated in FRP casing and were attached on the concrete's surface with epoxy resin.

Thermal FBG sensors were also installed on both bridges, to ensure the measurements' independence from the sensors' temperature dependences.

Instrumentation of a 325tn Cantilever Crane, Newcastle, UK

The existing 250tn crane in Newcastle upon Tyne was designed and erected in 1936 by William Arrol & Co.

The crane consists of a double cantilever, with the shorter rear section carrying the ballast. The boom consists of a twin frame which is approximately 60m long.

The structure has recently undergone modernization to increase the load carrying capacity of the crane to 325tn at a radius of 80ft (24.2m).

The aim of the structural monitoring is to detect the strains at critical positions and compare them to the theoretical values.

Patch sensors installed on the upper and on the lower section of the main boom

Heavy duty cable conduits and sensor steel cover

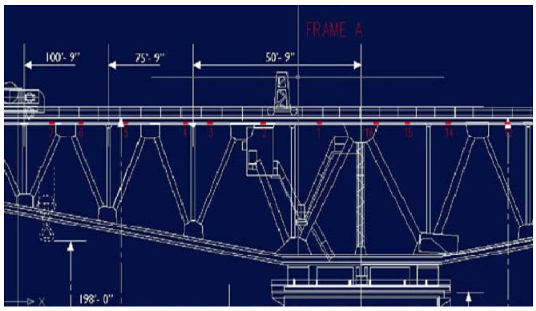

16 sensors along frame A of the central section

(Ευάγγελος Παστρεμένης, vastrin@crd.gr)

(Σημείωση Εκδότη: Η παραπάνω καταχώρηση είναι σαφώς διαφημιστική. Διαφημίζει, όμως, ένα πρωτοποριακό προϊόν, δημιουργημένο από Έλληνες Πολιτικούς Μηχανικούς, το οποίο αξίζει να το προβάλουμε.)

ΠΡΟΣΕΧΕΙΣ ΓΕΩΤΕΧΝΙΚΕΣ ΕΚΔΗΛΩΣΕΙΣ

Για τις παλαιότερες καταχωρήσεις περισσότερες πληροφορώες μπορούν να αναζητηθούν στα προηγούμενα τεύχη του «περιοδικού» και στις παρατιθέμενες ιστοσελίδες.

GenAmerica's 2016 3rd Panamerican Conference on Geosynthetics, 11 – 14 April 2016, Miami Beach, USA, www.geoamericas2016.org

International Symposium on Submerged Floating Tunnels and Underwater Structures (SUFTUS-2016), 20-22 April 2016, Chongqing, China, www.cmct.cn/suftus

World Tunnel Congress 2016 "Uniting the Industry", April 22-28, 2016, San Francisco, USA, http://www.wtc2016.us

International Symposium "Design of piles in Europe - How did EC7 change daily practice?", 28-29 April 2016, Leuven, Belgium, www.etc3.be/symposium2016

7th In-Situ Rock Stress Symposium 2016 - An ISRM Specialised Conference, 10-12 May 2016, Tampere, Finland, www.rs2016.org

84th ICOLD Annual Meeting, 15-20 May 2016, Johannesburg, South Africa, www.icold2016.org

Infrastructure Summit 2016, 18 - 19 May 2016, London, United Kingdom, Ilya.Ryndin@emap.com

2nd International Conference on Rock Dynamics and Applications (RocDyn-2), 18 – 20 May 2016, Suzhou, China http://rocdyn.org

6th Annual Underground Infrastructure and Deep Foundations Qatar, 23–24 May 2016, Doha, Qatar, oliver.osea@iqpc.ae

13th International Conference Underground Construction Prague 2016 and 3rd Eastern European Tunnelling Conference (EETC 2016), 23 to 25 May 2016, Prague, Czech Republic, www.ucprague.com

GEOSAFE: 1st International Symposium on Reducing Risks in Site Investigation, Modelling and Construction for Rock Engineering - an ISRM Specialized Conference, 25 – 27 May 2016, Xi'an, China, www.geosafe2016.org/dct/page/1

14th International Conference of the Geological Society of Greece, 25-27 May, Thessaloniki, Greece, www.ege2016.gr

NGM 2016 - The Nordic Geotechnical Meeting, 25 - 28 May 2016, Reykjavik, Iceland, www.ngm2016.com

International Mini Symposium Chubu (IMS-Chubu) New concepts and new developments in soil mechanics and geotechnical engineering, 26 - 28 May 2016, Nagoya, Aichi, Japan, www.jiban.or.jp/index.php?option=com_content&view=article&id=1737:2016052628&catid=16:2008-09-10-05-02-09&Itemid

11th HSTA< International Congress on Mechanics – Mini-Symposium Computational Geomechanics from Micro to Macro, May 27-30, 2016, Athens, Greece, http://11hstam.ntua.gr

19SEAGC – 2AGSSEAC Young Geotechnical Engineers Conference, 30th May 2016, Petaling Jaya, Selangor, Malaysia, seagc2016@gmail.com

19th Southeast Asian Geotechnical Conference & 2nd AGSSEA Conference Deep Excavation and Ground Improvement, 31 May – 3 June 2016, Subang Jaya, Malaysia, seagc2016@gmail.com

ISSMGE TC211 Conference Session within the framework of the 19th Southeast Asian Geotechnical Conference "GROUND IMPROVEMENT works: Recent advances in R&D, design and QC/QA"

ISL 2016 12th International Symposium on Landslides Experience, Theory, Practice, Napoli, June 12th-19th, 2016, www.isl2016.it

BCRRA 2017 Tenth International Conference on the Bearing Capacity of Roads, Railways and Airfields, 28 –30 June 2017, Athens, Greece, www.bcrra2017.com

ICONHIC 2016 1st International Conference on Natural Hazards and Infrastructure: Protection, Design, Rehabilitation, 28-30 June 2016, Chania, Greece, http://iconhic2016.com

ICONHIC 2016 Performance-based soil-structure interaction of lifelines and infrastructure, gerolymos@gmail.com, asextos@civil.auth.gr & a.sextos@bristol.ac.uk

4th GeoChina International Conference Sustainable Civil Infrastructures: Innovative Technologies for Severe Weathers and Climate Changes, July 25-27, 2016, Shandong, China, http://geochina2016.geoconf.org

S3: Slopes, Slides and Stabilization, August 1-3, 2016, Denver, USA, events@dfi.org

6th International Conference on Recent Advances in Geotechnical Earthquake Engineering and Soil Dynamics August 1-6, 2016, Greater Noida (NCR), India, www.6icragee.com

EUROC 2016 - ISRM European Regional Symposium Rock Mechanics & Rock Engineering: From Past to the Future, 29-31 August 2016, Ürgüp-Nevşehir, Cappadocia, Turkey http://eurock2016.org

ICEGE 2016 1st International Conference on Energy Geotechnics, 29-31 August 2016, Kiel, Germany, www.iceg-2016.de

3rd ICTG – 3rd International Conference on Transportation Geotechnics 4 - 7 September 2016, Guimaraes, Portugal, www.civil.uminho.pt/3rd-ICTG2016

IAS'5 5th International Conference on Geotechnical and Geophysical Site Characterisation, 5-9 September 2016, Gold Coast, Queensland, Australia, http://www.isc5.com.au

The World Multidisciplinary Earth Sciences Symposium– WMESS 2016, 5-9 September 2016, Prague, Czech Republic www.mess-earth.org

ACCUUS 2016 15th World Conference Underground Urbanisation as a Prerequisite for Sustainable Development, September 12-15, 2016, http://acuus2016.com

SAHC 2016 - 10th international Conference on Structural Analysis of Historical Constructions 13-15 September 2016, Leuven, Belgium, www.sahc2016.be

13 Baltic States Geotechnical Conference Historical Experiences and Challenges of Geotechnical Problems in Baltic Sea Region, 15 - 17 September 2016, Vilnius, Lithuania, http://www.13bsgc.lt

ACE 2016 12th International Congress on Advances in Civil Engineering, 21-23 September 2016, Istanbul, Turkey, http://www.ace2016.org

EuroGeo 6 – European Regional Conference on Geosynthetics, 25 – 29 Sep 2016, Istanbul, Turkey, www.eurogeo6.org

8th Nordic Grouting Symposium State of the art – Future Development, 26-27 September 2016, Oslo, Norway, http://nordicgrouting.com

5th International Scientific Conference on Industrial and Hazardous Waste Management, 27 - 30 September 2016, Chania, Crete, Greece, http://hwm-conferences.tuc.gr

2nd International Specialized Conference on Soft Rocks – ISRM 2016 Understanding and interpreting the engineering behavior of Soft Rocks, 6-7 October 2016, Cartagena, Colombia, www.scg.org.co/?p=1634

ARMS 9, 9th Asian Rock Mechanics Symposium, ISRM Regional Symposium, 18-20 October 2016, Bali, Indonesia, http://arms9.com

SFGE 2016 Shaping the Future of Geotechnical Education International Conference on Geo-Engineering Education 20 - 22 October 2016, Minascentro, Belo Horizonte, MG, Brazil, http://cobramseg2016.com.br/index.php/sfge-sobre/?lang=en

10th ICOLD European Club Symposium & Exhibition, 25-30 October 2016, Antalya, Turkey, http://trcold.com

3-5 November 2016, Santorini, Greece
http://nemo.conferences.gr

150 years ago, in early January 1866, the first precursory phenomena (earthquakes, gas leaks, coast sinking) signified the beginning of the 6th and largest subaerial eruption of the Kamenis volcano.

This eruption will last until October 1870 and will build up the biggest part of today's Nea Kameni island. However, the most interesting characteristic of this eruption was not in its size, length, type or the depositional mechanisms of the volcanic products. What makes this eruption exceptionally interesting is the level of development of natural, historical and social sciences at the time of its occurrence which, in conjunction with the political and social environment in Europe at the time, causes international interest and coincides with, or creates, a series of events that will play an important role in the development of sciences and Santorini itself.

During the multiple events of 1860, the construction of the Suez Canal, the communication boost, the expansion of imperialist forces in the Mediterranean and the rest of the world, the Cretan revolution and the blow-up of Arkadi monastery in 1866, the struggles of Egypt and Algeria, the Eastern Question and the dissolution of the Ottoman Empire, two very important events take place in Santorini. The first is the volcanic eruption of 1866, and second is the discovery of the prehistoric buildings in Thirasia, which was brought by the intense exploitation of the Theran pumice quarries for the hydraulic projects of the Mediterranean. These indicents created a major international interest which attracted scientists, diplomats and military to the island.

It is the infant period for geosciences, mainly of the branches of general Geology and Paleontology. Archaeology is linked with these sciences through the ongoing paleolithic excavations in France and Spain.

The detailed observation, study and recording of the eruption of 1866-1870, the study of the structure of the Santorini volcanoes and the excavations in Thera and Therasia at the same time, constitute a methodological culmination of new dynamic sciences. The tephra layers and their stratigraphic sequence, the buildings and the findings that date them, the use of chemical methods, the evolutionism and positivism, are science innovations that spread between the waves caused by the warships and the rival European imperialist powers.

The archaeological discovery of the Late Cycladic house in Therasia under the ashes (aspa) is realized with the use of novel for the period technological methods. Under the noise of the Kameni eruptions, a breakthrough collaboration between geologists and archaeologists develops, one of the first cases of interdisciplinary cooperation and joint evaluation approach. The Cycladic house was initially excavated by Nomikos and Alafouzos, followed shortly after by Fouque accompanied by the French and Greek scientific committee. This first excavation of Therasia paved the way for the following prehistoric excavations for the Aegean, as it occured before Troy, Knossos and Mycenae.

During the same period, the study of the geological structure of Santorini has led Fouque to adopt the dialectic – evolutionary thinking method and employ it for the interpretation of the evolution of the area, a very important step for geological thinking.

For a few years, Thera and Therasia exhibited acute and concentrated activities, asking for their explanation and integration to the historical and epistemological framework. These phenomena revealed the evolution paths and explosive development of epistemological forms and modes, within the generalised series of conflicts in the Eastern Mediterranean.

For all the previous reasons, it was decided to organize the NEMO 2016 International Conference in order not only to highlight the aforementioned conjunction of events, but also to demonstrate the path towards scientific maturity, the fields of interest, the political forces that were in the spotlight, the economic hopes and the new social forces and teams that were developed within the general framework (collectors, travelers, schools, monastic orders…). The Conference aims to bring into site the above issues through interdisciplinarity, highlighting the accomplishments of Geological, Volcanological, Historic-Archaeological and Social Sciences in Santorini, from 1866 until present.

Topics

Science and Santorini in the 19th century

- The conceptual framework of earth and humanistic sciences in the middle of 19th century
- Santorini's social and economic structure during the 1866 eruption
- The 1866-1870 eruption through the observations, descriptions, recordings and studies of the "contemporary"

in situ studiers – researchers. The application of novel scientific methods for the study of volcanic gases and rocks
- Santorini's historical eruptions and social life through the archives of the voyagers, scientists and the Therean studiers – researchers

Science and Santorini today

- Earth sciences and volcanoes, since 1866 till present. The contribution of the Santorini volcanological studies in their evolution
- Archaeology and Volcanology – volcanoes and civilization: the Santorini case and worldwide analogues
- Archaeological excavations in Thera and Therasia
- Study and monitoring of Santorini volcanoes before and after the 2011-2012 crisis: estimations and conclusions

Volcanoes – Culture and Society

- Timeless island civilizations and cultures
- Myths, legends, way of life and arts
- Local societies: volcanic hazard, social impacts and survival strategies
- Volcanoes and sustainable development: raw materials, products, energy, tourism
- Protection of the volcanic environment: human establishments / natural resources
- Architectural and Archaeological heritage

Contact

Heliotopos Conferences
Imerovigli, GR-84700 Santorini, Greece
Phone: +30 2286023670, 24758, Fax: +30 2286023672
E-mail: conf@heliotopos.net

GeoAsia 6 - 6th Asian Regional Conference on Geosynthetics 8-11 November 2016, New Delhi, India, http://seags.ait.asia/news-announcements/11704

RARE 2016 Recent Advances in Rock Engineering 16-18 November 2016, Bangalore, India, www.rare2016.in

TBM DiGs Istanbul 2016 2nd International conference on "TBM DiGs in difficult grounds", 16-18 November 2016, Istanbul, Turkey, www.tbmdigsturkey.org

International Symposium on Submerged Floating Tunnels and Underwater Tunnel Structures (SUFTUS-2016), 16—18 December 2016, Chongqing, China, www.cmct.cn/suftus

AfriRock 2017, 1st African Regional Rock Mechanics Symposium, 12 – 17 February 2017, Cape Town, South Africa, www.saimm.co.za/saimm-events/upcoming-events

World Tunnel Congress 2017
Surface challenges – Underground solutions
9 to 16 June 2017, Bergen, Norway
www.wtc2017.no

"Surface problems – Underground solutions" is more than a slogan; for ITA-AITES and its members it is a challenge and commitment to contribute to sustainable development. The challenges are numerous and the availability of space for necessary infrastructure ends up being the key to good solutions. The underground is at present only marginally utilized. The potential for extended and improved utilization is enormous.

Rapid population growth, increased urbanisation and climate change in the decades ahead will require major infrastructure investments and wide use of underground solutions.

Urbanisation encourage underground solutions

For the first time in history, more than half of the world's population live in cities. The lack of new urban space means that infrastructure must be planned underground. Accordingly, the use of the underground needs to be carefully and coherently engineered with sustainability in mind.

New infrastructure must take into account, that future tunnels and underground facilities must be employed to protect critical infrastructure from the forces of nature and human interference. Strategic assets for oil and gas, information technology and communications, and civil defence are increasingly being housed in extremely secure locations, such as large rock caverns. This ensures their operability even when disaster strikes.

More renewables necessary

Climate mitigation may be important, but climate solutions are even more so. Norway is even today a major supplier in the renewable energy network thanks to the high number of Hydro Electric Power plants. The demand for more green energy is sought-after all over the world and Norway have this expertise.

"Surface challenges – Underground solutions" is more than a slogan; for ITA-AITES and its members it is a challenge and commitment to contribute to sustainable development. The challenges are numerous and the availability of space for necessary infrastructure ends up being the key to good solutions. The underground is at present only marginally utilized. The potential for extended and improved utilization is enormous.

Topics

1. Site investigation, ground characterization
2. Urban tunneling (planning, design and construction)
3. Strategic use of underground space for resilient city growth

4. Utilization of underground for hydropower projects (unlined tunnels and shafts, underwater piercing, air cushion chambers)
5. Mechanized excavation (hard rock, soft rock and soil)
6. Innovations in drill and blast excavation
7. Large caverns (planning, design and construction)
8. Underwater tunnels (strait crossings for road and railway, utility tunnels)
9. Tunnelling for mining purposes
10. Underground waste storage and disposal
11. Innovations in rock support and water proofing technology
12. Operation, surveillance and maintenance
13. Safety management of complex underground excavations
14. Stability assessment, risk analysis and risk management
15. Seismic design of tunnels and underground excavations
16. Tunnel refurbishment
17. Case histories – lessons learnt

Contact

Appointed Professional Congress Organizer:

Travel Planners of Scandinavia A/S
Conrad Mohrsvei 11, N-5068 Bergen, Norway / Enterprise
http://www.travel-planners.no
Harald Riisnaes
Managing Director & Owner
harald.riisnaes@travel-planners.no
Tel: +47 55 23 00 70

EUROCK 2017
Human Activity in Rock Masses
13-15 June 2017, Ostrava, Czech Republic
www.eurock2017.com

On behalf of the organizing committee I am delighted to invite you to participate in the 2017 ISRM European Rock Mechanics Symposium (EUROCK 2017) to be held in Ostrava, Czech Republic, on June 19-22, 2017. This Symposium is the common endeavour of the Institute of Geonics of the Czech Academy of Sciences and the Czech National Group of the ISRM, who are doing their best to organize a pleasant and valuable event.

We have prepared an appealing program with a good number of keynote lectures by some of the world's leading experts on rock mechanics. Three short workshops will also take place before the Symposium and some visits to different attractive mine and civil engineering works are in preparation for the aftermath.

You will also have the opportunity to visit our town and region. The Moravian-Silesian Region is located in the most eastern part of the Czech Republic, about 300 km as the crow flies from the centre of Prague. However, it is only 1 hour by air, 3 hours by rail and 4 hours by road. Ostrava, the third largest city in the Czech Republic and the heart of the Moravian-Silesian Region, is located in the north-eastern part of the country. It is situated near the Slovak and Polish border on the banks of the Ostravice River overlooking the beautiful mountains of Beskydy. Ostrava has only recently lost the face of a typically industrial city. The coal mining finally ended there in 1994. The industrial heritage is a unique jewel of architecture. Instead of original mines, there are mining museums now and there are a number of closed metallurgical buildings waiting to be innovatively reused. Besides the technical heritage, the city offers its visitors many cultural and historical attractions, as well as other sights that allow tourists to enjoy a pleasant day full of exceptional experiences. You can look forward to experiencing the legendary Czech hospitality, as well as the excellent Czech cuisine. You will fall in love with the taste and aroma of known and unknown specialties typical of this region.

It is a special honour for me to host the Symposium EUROCK for the second time in the Czech Republic after the event in 2005 (EUROCK 2005 in Brno city) and I strongly hope that an exciting program and the charms of this beautiful central part of Europe will contribute to make the Symposium a successful and unforgettable event.

I am looking forward to meeting you in Ostrava in June 2017.

Yours sincerely,

Petr Konicek
Chairman of the organizing committee
Department of Geomechanics and mining research

Institute of Geonics of the Czech Academy of Sciences
Ostrava, Moravian-Silesian Region, Czech Republic

Topics

- Rock mass properties
- Laboratory and in-situ rock testing
- Mine design and ground control
- Underground storage and waste disposal
- Dynamic phenomena in rock mass
- Design methodology in mining and underground constructions
- New materials and technologies in geomechanics and geotechnics
- CO_2 sequestration
- Geothermal energy
- Rock disintegration
- Rock mass issues in mine closure
- Preservation of natural stones

Short Courses and Workshops

One-day workshops will be organized before the Symposium (19 June 2017). The following areas of research will be presented:

- Workshop on Destress blasting in rock mass
- Workshop on X-ray computed tomography in geosciences
- Workshop on Utilization of water jets for exploitation and processing of geomaterials

CONTACTS

Organizing committee
Dr. Petr Konicek
Institute of Geonics AS CR
Studentska 1768

708 00 Ostrava - Poruba
Czech Republic

P.: +420 596 979 224
F.: +420 596 919 452
E.: info@eurock2017.cz

Symposium Secretariat

BOS. org Ltd.
FN Ostrava - Domov sester
17. listopadu 1790/5
708 52 Ostrava - Poruba
Czech Republic
P.: +420 595 136 808
F.: +420 475 205 169
E.: ostrava@bos-congress.cz

BCRRA 2017
Tenth International Conference on the Bearing Capacity of Roads, Railways and Airfields

28th to 30th June 2017, Athens, Greece
www.bcrra2017.com

BCRRA 2017 Conference will cover aspects related to materials, laboratory testing, design, construction, maintenance and management systems of transport infrastructure focusing on roads, railways and airfields. Additional aspects that concern new materials and characterization, alternative rehabilitation techniques, technological advances as well as pavement and railway track substructure sustainability will be included. Providing a unique opportunity to interact and exchange and share information amongst researchers, practicing engineers and other professionals, BCRRA 2017 will welcome experts in the field from all over the world who can exchange their views and experiences, and have an outlet to discuss new concepts and innovative solutions.

Topics

The Conference will include aspects of transportation infrastructure focusing on roads, railways and airfields. Topics will concentrate but not limit to the following:

1. Policies on the bearing capacity of roads, railways and airfields
2. Unbound aggregate materials and soil properties
3. Bound materials characteristics, mechanical properties and testing
4. Traffic loading
5. Field measurement techniques and analysis tools
6. Pavement field evaluation
7. Correlation of laboratory and field testing results
8. Monitoring and assessment of roads, railways and airfields structures
9. Geophysical methods for structural evaluation
10. Pavement surface condition and performance assessment
11. Maintenance and preservation
12. Reinforcement and rehabilitation design
13. Analysis of Long-Term Pavement Performance (LTPP) data
14. Drainage and environmental effects
15. Climate change, energy and sustainability
16. Full scale testing (ALF, HVS)
17. Emerging technologies
18. Life cycle analysis
19. Non-standard pavements
20. Case histories of roads, railways and airfields

Contact Us

For abstract/paper submission issues and scientific matters:

Dr. Christina Plati
Konstantina Georgouli
(+30) 210 7721328
pavnet@central.ntua.gr

For registration, accommodation and venue matters:

Conference Secretariat

16 Kifisias Av., GR-11526, Ampelokipi
Georgia Kateriniou
(+30) 210 7499318 ,7499300
secretariat@bcrra2017.com

GeoMEast2017, 15 - 19 July 2017, Sharm El-Sheik, Egypt, www.geomeast2017.org

19th International Conference on Soil Mechanics and Geotechnical Engineering, 17 - 22 September 2017, Seoul, Korea, www.icsmge2017.org

GeoAfrica 2017
3rd African Regional Conference on Geosynthetics

9 – 13 October 2017, Morocco

11th International Conference on Geosynthetics (11ICG)

16 - 20 Sep 2018, Seoul South Korea
csyoo@skku.edu

10th Asian Rock Mechanics Symposium - ARMS10
October 2018, Singapore

Prof. Yingxin Zhou
Address:
1 Liang Seah Street
#02-11 Liang Seah Place
SINGAPORE 189022
Telephone: (+65) 637 65363
Fax: (+65) 627 35754
E-mail: zyingxin@dsta.gov.sg

AFTES International Congress "The value is Underground"
13-16 November 2017, Paris, France

Contact
AFTES
15, rue de la Fontaine au Roi FR-75011 Paris France
Tel. +33 1 44 58 27 43
Fax +33 1 44 58 24 59
Email aftes@aftes.fr
Website www.aftes.asso.fr

World Tunnel Congress 2018
20-26 April 2018, Dubai, United Arab Emirates

Contact
P.O. Box: 4484
ENOC Building # 1 , 2nd Floor, Wing A
Oud Metha Street
Dubai
Tel. +971 4 337 4449
Fax +971 4 337 2228
Email dxbsoe@emirates.net.ae
Website www.uaesocietyofengineers.com

EUROCK 2018
22-26 May 2018, Saint Petersburg, Russia

Contact Person: Prof. Vladimir Trushko
Address: 21-st line V.O., 2
199106 St. Petersburg
Russia
Telephone: +7 (812) 328 86 71
Fax: +7 (812) 328 86 76
E-mail: trushko@spmi.ru

UNSAT2018 The 7th International Conference on Unsaturated Soils, 3 - 5 August 2018, Hong Kong, China, www.unsat2018.org

ARMS10
10th Asian Rock Mechanics Symposium
ISRM Regional Symposium
October 2018, Singapore

Contact Person: Prof. Yingxin Zhou
Address: 1 Liang Seah Street
#02-11 Liang Seah Place
SINGAPORE 189022
Telephone: (+65) 637 65363
Fax: (+65) 627 35754
E-mail: zyingxin@dsta.gov.sg

14th ISRM International Congress
2019, Foz de Iguaçu, Brazil

Contact Person: Prof. Sergio A. B. da Fontoura
E-mail: fontoura@puc-rio.b

ecsmge-2019

The 17th European Conference on Soil Mechanics and Geotechnical Engineering "Geotechnical Engineering, foundation of the future"

1st - 6th of September 2019, Reykjavik, Iceland

www.ecsmge-2019.com

The theme of the conference embraces all aspects of geotechnical engineering. Geotechnical engineering is the foundation of current as well as future societies, which both rely on complex civil engineering infrastructures, and call for mitigation of potential geodangers posing threat to these. Geotechnical means and solutions are required to ensure infrastructure safety and sustainable development. Those means are rooted in past experiences enhanced by research and technology of today.

At great events such as the European Geotechnical Conference we should: Spread our knowledge and experience to our colleagues; Introduce innovations, research and development of techniques and equipment; Report on successful geotechnical constructions and application of geotechnical design methods, as well as, on mitigation and assessment of geohazards and more.

Such events also provide an opportunity to draw the attention of others outside the field of geotechnical engineering to the importance of what we are doing, particularly to those who, directly or indirectly, rely on our services, knowledge and experience. Investment in quality geotechnical work is required for successful and safe design, construction and operation of any infrastructure. Geotechnical engineering is the key to a safe and sustainable infrastructure and of importance for the society, economy and the environment. This must be emphasized and reported upon.

ΕΝΔΙΑΦΕΡΟΝΤΑ ΓΕΩΤΕΧΝΙΚΑ ΝΕΑ

Landslides (videos)

Biggest landslides worldwide
Part 1 https://www.youtube.com/watch?v=iciLigLgsWc,
Part 2 https://www.youtube.com/watch?v=r4_yhypLuVQ
(Published on Sep 2, 2013)

World's Most Killer Landslides Ever Recorded
https://www.youtube.com/watch?v=VJ_ykqJuGI0
(Published on Jan 8, 2015)

Larger Than Life Landslide

In 1980, the eruption of Mount St. Helen's created a landslide so powerful that it leveled 150 acres of forest and killed 57.

https://www.youtube.com/watch?v=K5pidzTZslo

(Published on Mar 9, 2012).

Ropoto: Greece's Sinking Ghost Town (video)

Ropoto was a thriving village and home to 300 families, until an unprecedented disaster in 2012 turned it into a ghost town, today forgotten by authorities.

Με τις νέες φωτογραφίες του χωριού Ροπωτό, ασχολείται το ρωσικό δίκτυο Russia Today, λόγω της εκτεταμένης κατολίσθησης η οποία έχει ξεκινήσει από το 2012, καταδεικνύοντας τις καταστροφικές συνέπειες της φύσης στην άλλοτε ακμάζουσα κοινότητα.

Το χωριό Ροπωτό, στην περιοχή των Τρικάλων στην κεντρική Ελλάδα, έχει πλέον εγκαταλειφθεί όταν οι χωρικοί αναγκάστηκαν να εγκαταλείψουν τα σπίτια τους εξαιτίας των συνεχιζόμενων κατολισθήσεων, αναφέρει το ρωσικό πρακτορείο ειδήσεων.

Πολλά κτίρια έχουν καταρρεύσει εντελώς, ενώ άλλα φαίνεται να παραμένουν σε μεγάλο βαθμό ανέπαφα. Το έδαφος είναι σαθρό, και σύμφωνα με πρόσφατο ντοκιμαντέρ απεικονίζεται η δεινή κατάσταση των πληγέντων κατοίκων.

Περισσότερες από 300 οικογένειες αναγκάστηκαν να εγκαταλείψουν τα σπίτια τους λόγω της απότομης μετατόπισης του εδάφους, και δεν έχουν λάβει καμία βοήθεια ή αποζημίωση από την ελληνική κυβέρνηση, σύμφωνα με κατοίκους της περιοχής και συνέντευξη τους σε πρόσφατο ντοκιμαντέρ ελληνικών ΜΜΕ.

«Το χωριό δεν υπάρχει πια. Οι άνθρωποι δεν μπορούν να ζήσουν εκεί» είπε κάτοικος. Ο ίδιος ισχυρίστηκε τίποτα δεν έγινε τίποτα απολύτως για να διοχετεύσουν το νερό της βροχής μακριά ή να προστατεύσουν τα σπίτια, και οι κάτοικοι αφέθηκαν στην τύχη τους.

Ο ίδιος είπε επίσης στους δημοσιογράφους ότι οι κάτοικοι εξακολουθούν να πληρώσουν φόρο ακίνητης περιουσίας (ΕΝΦΙΑ), παρά την δομική επιδείνωση των σπιτιών τους!!!!

Δεν είναι η πρώτη φορά κατά την οποία διαπιστώνεται το ανάλγητο πρόσωπο της εξουσίας σε ένα χωριό το οποίο επέζησε από την εποχή της τουρκοκρατίας μέχρι τις ημέρες μας.

Η Νομαρχία, ο Δήμος, η Περιφέρεια και τέλος όλες οι κυβερνήσεις άφησαν το χωριό αυτό να το «πάρει το ποτάμι».

Την ίδια στιγμή απαιτούν να λαμβάνουν φόρο σαν ν μην συμβαίνει τίποτα. Μόνο στην Ελλάδα συμβαίνουν αυτές οι συμπεριφορές διότι πολλοί ξεχάσαν να ασχοληθούν και με τους κατοίκους της ελληνικής υπαίθρου.

ΤΟ ΒΙΝΤΕΟ : https://youtu.be/uVOAqKrACZU?t=15

https://www.youtube.com/watch?v=Ur8v6QBFVO8&ebc=ANyPxKrIEfJMSt76fRvteE-0syKw_yYzzbF1Ju05wwOh-UTvptraqzDMFhMc85sDYxaIGKy0eYAGQaNvZmtNJo5-CuAo3C8iDg (πλήρες)

10 αξιοθέατα που βρίσκονται κάτω από τη γη!

Ορισμένοι από τους πιο εντυπωσιακούς προορισμούς στον κόσμο είναι κρυμμένοι κάτω απ' τα πόδια μας. Κάποιοι είναι θαύματα της φύσης, άλλοι δημιουργήματα του ανθρώπου, όλα όμως αξίζουν να βγούμε από τον δρόμο μας και να κατεβούμε πολύ χαμηλά.

1. Μετρό Στοκχόλμης

Το μετρό της Στοκχόλμης θεωρείται το ωραιότερο στην Ευρώπη και το αποκαλούν «η μακρύτερη γκαλερί στον κόσμο», αφού κάθε σταθμός είναι διακοσμημένος με εντυπωσιακά παλιά και σύγχρονα έργα τέχνης από περισσότερους από 150 δημιουργούς. Από τους 100 σταθμούς οι 47 είναι υπόγειοι, ενώ οι εφτά γραμμές ξεχωρίζουν με χρώματα «παλαιότητας»: οι πράσινοι σταθμοί εγκαινιάστηκαν το 1950, οι κόκκινοι το 1964 και οι μπλε είναι οι νεότεροι (1974) και βρίσκονται στο βαθύτερο σημείο κάτω από την πόλη.

2. Ναός σε αλατωρυχείο, Πολωνία

Στον ναό που κατασκευάστηκε στα βάθη του αλατωρυχείου Wieliczka στην Πολωνία, τα πάντα, από τους πολυελαίους ως την Αγία Τράπεζα, έχουν λαξευτεί σε ορυκτό αλάτι. Οι ξεναγήσεις εδώ ξεκίνησαν τον 14ο αιώνα και ανάμεσα σε αυτούς που κατέβηκαν 200μ. κάτω απ' το έδαφος για να το θαυμάσουν, ήταν από τον Κοπέρνικο και τον Γκαίτε ως τον Τζορτζ Μπους επί προεδρίας των ΗΠΑ. Ένα άλλο τμήμα του ορυχείου έχει διαμορφωθεί σε αίθουσα εκδηλώσεων (επιδείξεις μόδας, συναυλίες κ.ά).

3. Βασιλική Κινστέρνα, Κωνσταντινούπολη

Η Βασιλική Κινστέρνα είναι μια υπόγεια δεξαμενή – αρχιτεκτονικό θαύμα από την εποχή του Ιουστινιανού και μια από τις πιο ατμοσφαιρικές γωνιές της Κωνσταντινούπολης. Οι Τούρκοι την αποκαλούν «Βυθισμένο Παλάτι» (Yerebatan Sarayi) και όντως αυτή είναι η εντύπωση που αποκομίζει κάποιος βλέποντας τους 336 υποβλητικά φωτισμένους κίονες να αναδύονται από το νερό σε 12 σειρές, υπό τους ήχους κλασικής μουσικής.

4. Σταθμός Formosa Boulevard, Ταϊβάν

Στην οροφή του σταθμού Formosa Boulevard, στην Ταϊβάν, υπάρχει μια εγκατάσταση που αποτελείται από 4.500 κομμάτια γιαλού. Θεωρείται το μεγαλύτερο γυάλινο έργο τέχνης στον κόσμο και με τους φαντασμαγορικούς χρωματισμούς και τα οπτικά εφέ που δημιουργεί το φως, ο χώρος είναι τόσο ατμοσφαιρικός που χρησιμοποιείται και για γαμήλιες τελετές.

5. Βαθύτερο θεματικό πάρκο, Ρουμανία

Το βαθύτερο θεματικό πάρκο του κόσμου έχει στηθεί μέσα στα αρχαία αλατωρυχεία Salina Turda, στην Τρανσυλβανία της Ρουμανίας. Οι επισκέπτες κατεβαίνουν σχεδόν 122 μέτρα για να ανακαλύψουν την ιστορία του αλατιού, να ανέβουν στον μύλο του λούνα παρκ, να παίξουν μίνι γκολφ, μπάσκετ, μπόουλινγκ και πινγκ πονγκ ή να κάνουν βαρκάδα στο σπήλαιο με τους εντυπωσιακούς σταλακτίτες και σταλαγμίτες.

6. Σπήλαιο Hang Son Doong, Βιετνάμ

Το μεγαλύτερο σπήλαιο στον κόσμο βρίσκεται στο Βιετνάμ κι ενώ θεωρείται ότι σχηματίστηκε πριν από 2 εκατομμύριο χρόνια, το ανακάλυψε τυχαία ένας αγρότης μόλις το 1991. Πρόκειται βέβαια για το Χανγκ Σον Ντόνγκ (Hang Son Doong), το οποίο στην αχανή του έκταση με τα χιλιάδες μυστήρια που κρύβει, ανακαλύφθηκε πως έχει δική του ζούγκλα, ένα ποτάμι, εξωπραγματικές ακτές και σταλαγμίτες 70 μετρων. Η εξερεύνηση δεν έχει ολοκληρωθεί ακόμα από τους ειδικούς, ωστόσο υπάρχει μια διαδρομή για τουρίστες οι οποίοι μπαίνουν με το σταγονόμετρο: στη διάρκεια του 2015 επιτράπηκε η είσοδος μόνο σε 500 επισκέπτες.

7. Πλωτό υπόγειο ποτάμι Puero Princesa, Φιλιππίνες

Ένα από τα «Νέα 7 Θαύματα της Φύσης» και υπό την προστασία της UNESKO από το 2004, το Puero Princesa είναι το μεγαλύτερο πλωτό υπόγειο ποτάμι στον κόσμο. Εχει μήκος 8 χλμ. που προσφέρουν στον επισκέπτη μια εξωτική εμπειρία περιήγησης στο θαυμαστό σύστημα σπηλαίων με εντυπωσιακούς σταλακτίτες, καταρράκτες, λίμνες με κρυστάλλινα νερά και απίθανη χλωρίδα και πανίδα.

8. Υπόγεια πόλη Coober Pedy, Αυστραλία

Χάρη στους 40 °C που τους ψήνουν καθημερινά, οι περισσότεροι κάτοικοι της Κούμπερ Πέντι, στη Νότια Αυστραλία, ζουν κάτω απ' τη γη. Αυτή είναι η μεγαλύτερη υπόγεια πόλη στον κόσμο, και «χτίστηκε» αξιοποιώντας στην ουσία τα ορυχεία που δημιουργήθηκαν την εποχή της εξόρυξης οπαλίου. Διαθέτει ένα πολύ καλό σύστημα εξαερισμού και διατηρεί σταθερή δροσερή θερμοκρασία, ενώ εκτός τα διαμερίσματα, στους «δρόμους» της συναντάς από βιβλιοπωλείο έως εκκλησία και ξενοδοχείο για όσους δεν αντιμετωπίζουν προβλήματα κλειστοφοβίας.

9. Μουσείο Cabinet War Rooms, Βρετανία

Κάτω από τους δρόμους του Λονδίνου, συγκεκριμένα κάτω από το Υπουργείο Οικονομικών, υπάρχει το μουσείο Cabinet War Rooms (ή Churchill War Rooms), Είναι αφιερωμένο στη ζωή του Βρετανού πρωθυπουργού Τσόρτιλ και οι αίθουσες αναπαριστούν με ακρίβεια το κέντρο διοίκησης της βρετανικής κυβέρνησης στη διάρκεια του Β' Παγκόσμιου Πολέμου.

10. Σπήλαιο Διρού, Λακωνία

Το σπήλαιο στη Βλυχάδα του Διρού στη Λακωνία, θεωρείται ένα από τα ομορφότερα σπήλαια στον κόσμο, αν και η 45λεπτη τουριστική διαδρομή με το καραβάκι στις θεματικές αίθουσές του, παρότι σε αφήνει με το στόμα ανοιχτό, δεν αποκαλύπτει όλα τα μυστικά του. Η παρουσία του νερού, η παντελής έλλειψη λάσπης, οι απίθανοι σχηματισμοί μέσα και έξω από το νερό, οι μοναδικές στον κόσμο «βελόνες» (καλύπτουν το μεγαλύτερο μέρος του και σχηματίζουν θύσανους) και τα συγκλονιστικά απολιθώματα ζώων, είναι μερικά από τα στοιχεία που συνιστούν το μεγαλείο του. Οι εξερευνήσεις δεν έχουν ολοκληρωθεί, καθώς οι σπηλαιολόγοι ανακαλύπτουν διαρκώς νέους θαλάμους.

(http://perierga.gr/2015/12, 14 Δεκεμβρίου 2015)

Vasquez Canyon: a new landslide in Santa Clarita, California

A significant landslide has developed in the last few days in Vasquez Canyon, in Santa Clarita in California. The landslide, which appears to be progressive and has no obvious recent trigger, has caused extensive buckling of the road, which has been closed over a three kilometre stretch. This image, from the Santa Clarita Valley Signal, provides quite a good general view of the situation beyond the road:

The landslide, from the Santa Clarita Valley Signal

The landslide has caused impressive damage to the highway:

Vasquez Canyon road from KTLA5

Interestingly, the media are suggesting that this buckling has occurred because the road is moving upwards. Whilst this might sound a little odd, this excellent drone footage suggests that this might the case:

This is a still from the drone footage of the landslides, showing the damage to the highway:

Vasquez Canyon Road via Youtube

This is Google Earth imagery of this section of the road, dated April 2015 – i.e. seven months ago:

Vasquez Canyon Road via Google Earth

There are clearly some signs of instability in this image, and note the other landslides in the image. The section of road that has failed is in a box cut, so it would appear that unloading of the slope may be a key factor in the landslide. And interestingly, this imagery from two years ago (May 2013) suggests significant movement at that time as well:

Vasquez Canyon road in 2013 from Google Earth

And finally, this is Google Street View imagery of the road, taken in 2011:

Vasquez Canyon road via Google street view

The extensive deformation in the road was clear even then – indeed the road shows longitudinal cracks along this entire section. Thus, although this landslide looks very sudden, it has been developing over a prolonged period.

(22 November 2015, http://blogs.agu.org/landslideblog/2015/11/22/vasquez-canyon-1)

Η εξέλιξη του φαινομένου

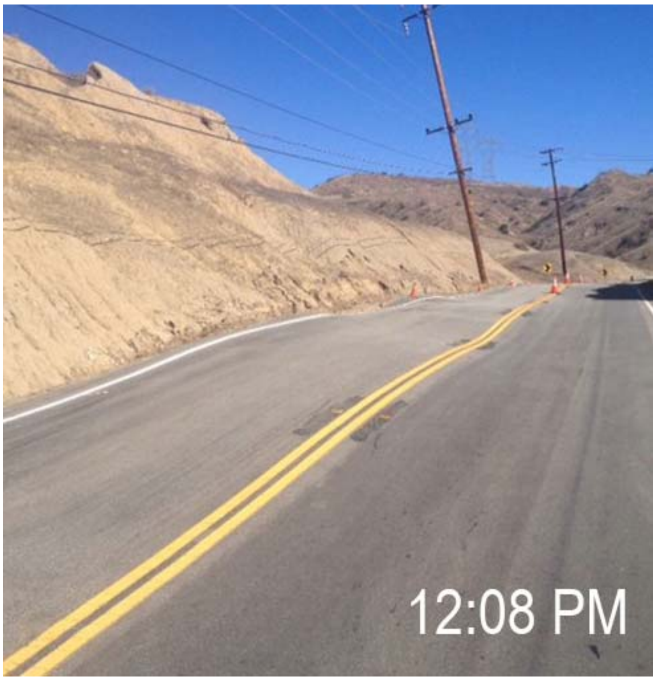

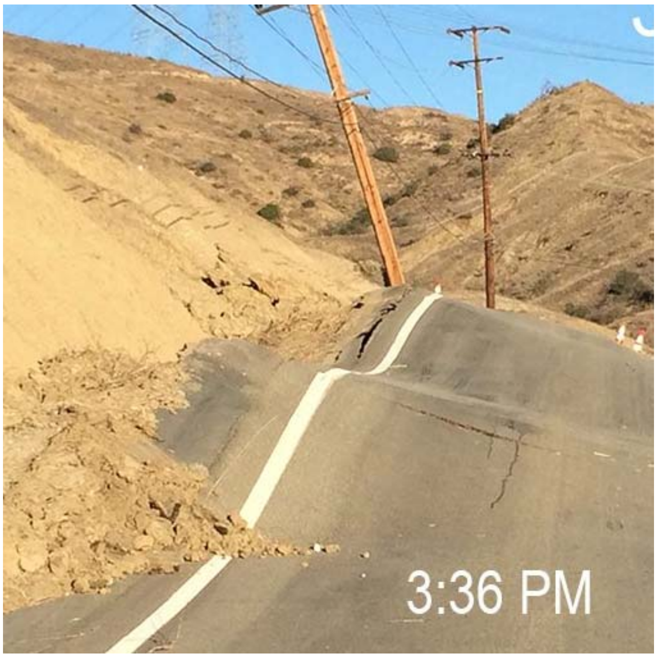

Η επόμενη φωτογραφία δείχνει τον ίδιο δρόμο, περίπου μία ώρα αργότερα, περίπου 16:30.

HUGE CRACK

ΕΝΔΙΑΦΕΡΟΝΤΑ - ΠΕΡΙΒΑΛΛΟΝ

Ανθρωπόκαινο
Ο άνθρωπος έχει φέρει τον πλανήτη «σε νέα γεωλογική εποχή»

Η Γη τη νύχτα όπως φαίνεται από τον Διεθνή Διαστημικό Σταθμό. Η ανθρώπινη παρουσία είναι παραπάνω από εμφανής.

Τα ανεξίτηλα ίχνη που αφήνει η ανθρώπινη δραστηριότητα στη Γη είναι πλέον τόσο ξεκάθαρα ώστε δικαιολογούν την αναγνώριση μιας νέας γεωλογικής εποχής, αναφέρει διεθνής ομάδα γεωλόγων.

Ο γεωλογικός χρόνος από το σχηματισμό της Γης μέχρι σήμερα χωρίζεται σε εποχές με βάση χαρακτηριστικά ευρήματα σε πετρώματα και ιζήματα. Σήμερα ζούμε επισήμως στην Ολόκαινο Εποχή, η οποία ξεκίνησε με τη λήξη της τελευταίας εποχής των παγετώνων πριν από 11.700 χρόνια.

Όλο και περισσότεροι γεωλόγοι πιστεύουν πλέον ότι το Ολόκαινο έχει ουσιαστικά λήξει και ο πλανήτης περνά στο Ανθρωπόκαινο, τη γεωλογική εποχή του ανθρώπου.

Η νέα εποχή δεν έχει αναγνωριστεί επίσημα και οι διαφωνίες παραμένουν ως προς την αποδοχή και τον ορισμό της: άλλοι πιστεύουν ότι το Ανθρωπόκαινο άρχισε με την διάδοση της γεωργίας τα τελευταία 10.000 χρόνια, ενώ άλλοι προτείνουν ως αρχή της την πρώτη δοκιμή πυρηνικής βόμβας, η οποία γέμισε τον πλανήτη με ίχνη ραδιοϊσοτόπων. Άλλοι, πάλι, θα προτιμούσαν να την ορίσουν με βάση τα μικροσκοπικά κομμάτια πλαστικού και άλλων τεχνητών υλικών που εντοπίζονται πλέον στα ιζήματα και τους πολικούς πάγους.

Στο τελευταίο τεύχος του περιοδικού Science, η Ομάδα Εργασίας Ανθρωπόκαινου, μια ομάδα εργασίας που συστάθηκε από την Διεθνή Επιτροπή Στρωματογραφίας, αναφέρει ότι οι ενδείξεις υπέρ της αναγνώρισης του Ανθρωπόκαινου είναι πλέον ξεκάθαρες.

Η Ομάδα Εργασίας συμφωνεί με τον ορισμό του Ανθρωπόκαινου με βάσει τα χαρακτηριστικά των σύγχρονων ιζημάτων: «Οι άνθρωποι επηρεάζουν το περιβάλλον από πολύ παλιά, πρόσφατα όμως υπήρξε μια ταχύτατη, παγκόσμια εξάπλωση νέων υλικών όπως το αλουμίνιο, το τσιμέντο και τα πλαστικά, υλικά που αφήνουν τα σημάδια τους στα ιζήματα» λέει ο Δρ Κόλιν Γουότερς της βρετανικής Γεωλογικής Υπηρεσίας, επικεφαλής της **μελέτης**.

«Η χρήση ορυκτών καυσίμων έχει διασπείρει σωματίδια τέφρας σε όλο τον κόσμο, κάτι που συμπίπτει χρονικά με την κορύφωση της διασποράς ραδιονουκλεοτιδίων από τις ατμοσφαιρικές δοκιμές πυρηνικών όπλων» συνεχίζει.

Η Ομάδα Εργασίας θα συνεχίσει να συλλέγει στοιχεία και το 2016 προκειμένου να δώσει συστάσεις για την αναγνώριση του Ανθρωπόκαινου και τον ορισμό του.

Προς το παρόν, πάντως, ζούμε ακόμα στο Ολόκαινο.

(Βαγγέλης Πρατικάκης / Newsroom ΔΟΛ, 08 Ιαν. 2016, http://news.in.gr/science-technology/article/?aid=1500050239)

The Anthropocene is functionally and stratigraphically distinct from the Holocene

C.N. Waters, J. Zalasiewicz, C. Summerhayes, A.D. Barnosky, C. Poirier, A. Gałuszka, A. Cearreta, M. Edgeworth, E.C. Ellis, M. Ellis, C. Jeandel, R. Leinfelder, J.R. McNeill, D. deB. Richter, W. Steffen, J. Syvitski, D. Vidas, M. Wagreich, M. Williams, A. Zhisheng, J. Grinevald, E. Odada, N. Oreskes, A.P. Wolfe

Evidence of an Anthropocene epoch

Humans are undoubtedly altering many geological processes on Earth—and have been for some time. But what is the stratigraphic evidence for officially distinguishing this new human-dominated time period, termed the "Anthropocene," from the preceding Holocene epoch? Waters *et al.* review climatic, biological, and geochemical signatures of human activity in sediments and ice cores. Combined with deposits of new materials and radionuclides, as well as human-caused modification of sedimentary processes, the Anthropocene stands alone stratigraphically as a new epoch beginning sometime in the mid–20th century.

Science, this issue p. 10.1126/science.aad2622

Structured Abstract

BACKGROUND

Humans are altering the planet, including long-term global geologic processes, at an increasing rate. Any formal recognition of an Anthropocene epoch in the geological time scale hinges on whether humans have changed the Earth system sufficiently to produce a stratigraphic signature in sediments and ice that is distinct from that of the Holocene epoch. Proposals for marking the start of the Anthropocene include an "early Anthropocene" beginning with the spread of agriculture and deforestation; the Columbian Exchange of Old World and New World species; the Industrial Revolution at ~1800 CE; and the mid-20th century "Great Acceleration" of population growth and industrialization.

ADVANCES

Recent anthropogenic deposits contain new minerals and rock types, reflecting rapid global dissemination of novel materials including elemental aluminum, concrete, and plastics that form abundant, rapidly evolving "technofossils." Fossil fuel combustion has disseminated black carbon, inorganic ash spheres, and spherical carbonaceous particles worldwide, with a near-synchronous global increase around 1950. Anthropogenic sedimentary fluxes have intensified, including enhanced erosion caused by deforestation and road construction. Widespread sediment retention behind dams has amplified delta subsidence.

Geochemical signatures include elevated levels of polyaromatic hydrocarbons, polychlorinated biphenyls, and pesticide residues, as well as increased $^{207/206}Pb$ ratios from leaded gasoline, starting between ~1945 and 1950. Soil nitrogen and phosphorus inventories have doubled in the past century because of increased fertilizer use, generating widespread signatures in lake strata and nitrate levels in Green-

land ice that are higher than at any time during the previous 100,000 years.

Detonation of the Trinity atomic device at Alamogordo, New Mexico, on 16 July 1945 initiated local nuclear fallout from 1945 to 1951, whereas thermonuclear weapons tests generated a clear global signal from 1952 to 1980, the so-called "bomb spike" of excess ^{14}C, ^{239}Pu, and other artificial radionuclides that peaks in 1964.

Atmospheric CO_2 and CH_4 concentrations depart from Holocene and even Quaternary patterns starting at ~1850, and more markedly at ~1950, with an associated steep fall in $\delta^{13}C$ that is captured by tree rings and calcareous fossils. An average global temperature increase of 0.6° to 0.9°C from 1900 to the present, occurring predominantly in the past 50 years, is now rising beyond the Holocene variation of the past 1400 years, accompanied by a modest enrichment of $\delta^{18}O$ in Greenland ice starting at ~1900. Global sea levels increased at 3.2 ± 0.4 mm/year from 1993 to 2010 and are now rising above Late Holocene rates. Depending on the trajectory of future anthropogenic forcing, these trends may reach or exceed the envelope of Quaternary interglacial conditions.

Biologic changes also have been pronounced. Extinction rates have been far above background rates since 1500 and increased further in the 19th century and later; in addition, species assemblages have been altered worldwide by geologically unprecedented transglobal species invasions and changes associated with farming and fishing, permanently reconfiguring Earth's biological trajectory.

OUTLOOK

These novel stratigraphic signatures support the formalization of the Anthropocene at the epoch level, with a lower boundary (still to be formally identified) suitably placed in the mid-20th century. Formalization is a complex question because, unlike with prior subdivisions of geological time, the potential utility of a formal Anthropocene reaches well beyond the geological community. It also expresses the extent to which humanity is driving rapid and widespread changes to the Earth system that will variously persist and potentially intensify into the future.

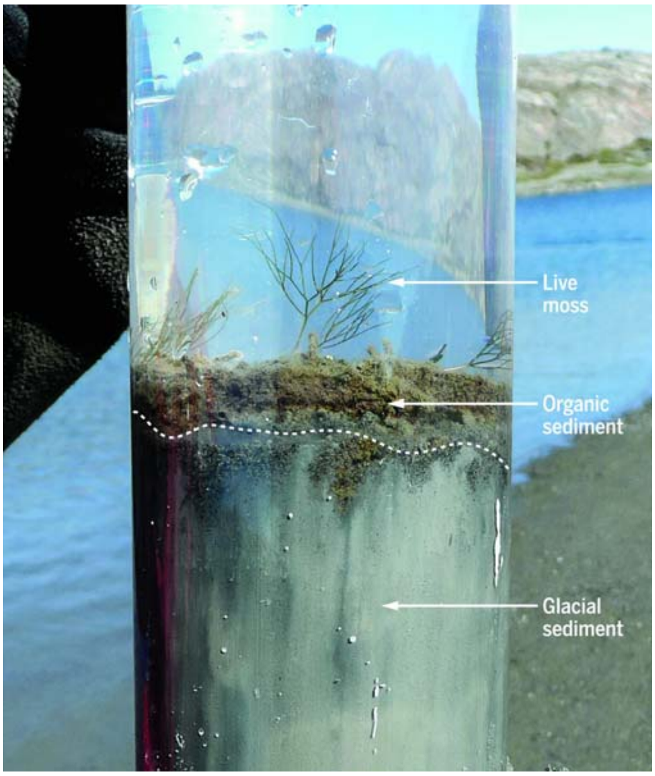

Indicators of the Anthropocene in recent lake sediments differ markedly from Holocene signatures.

These include unprecedented combinations of plastics, fly ash, radionuclides, metals, pesticides, reactive nitrogen, and consequences of increasing greenhouse gas concentrations. In this sediment core from west Greenland (69°03'N, 49°54'W), glacier retreat due to climate warming has resulted in an abrupt stratigraphic transition from proglacial sediments to nonglacial organic matter, effectively demarcating the onset of the Anthropocene. [Photo credit: J. P. Briner]

http://science.sciencemag.org/content/351/6269/aad2622

ΕΝΔΙΑΦΕΡΟΝΤΑ – ΛΟΙΠΑ

Τέσσερις (ελληνικές) γέφυρες - σημεία αναφοράς για το μέλλον

Αν ρωτήσεις έναν Έλληνα ποια είναι η πρώτη γέφυρα που του έρχεται στο μυαλό, οι απαντήσεις μάλλον θα διχαστούν ανάμεσα στη γέφυρα Ρίου-Αντιρρίου και... το γεφύρι της Αρτας. Η απόσταση ανάμεσα στις δύο γέφυρες είναι ίσως εκείνη που συμπυκνώνει και την ιστορία των δημοσίων έργων στη χώρα μας, με τα επιτεύγματα και τις κακοδαιμονίες του.

Η γεφυροποιία, πάντως, έχει σημαντική ιστορία στην Ελλάδα. Χωρίς να παραγνωρίζει κανείς την τέχνη των μαστόρων των λίθινων γεφυρών, το σύγχρονο κομμάτι της για πολλούς ξεκινά με τις πολύ «τολμηρές» γέφυρες που κατασκευάστηκαν επί εποχής Χαρίλαου Τρικούπη, στο πλαίσιο της ανάπτυξης του σιδηροδρομικού δικτύου. Η λίθινη τοξωτή γέφυρα Μάναρη, η μεγαλύτερη κοιλαδογέφυρα του είδους της στην Ελλάδα, και οι μεταλλικές γέφυρες στον Ασωπό Βοιωτίας και στον Μπράλο, με «άνοιγμα» 80 και 120 μέτρων αντίστοιχα, ήταν εξαιρετικά δείγματα της μηχανικής εκείνης της περιόδου. Οι περισσότερες όμως από τις μεγάλες γέφυρες εκείνης της εποχής δεν μακροημέρευσαν: καταστράφηκαν κατά τον Β΄ Παγκόσμιο Πόλεμο. Η κατασκευή μεγάλων γεφυρών ξεκινά και πάλι το 1960-65, και η περίοδος εκείνη έχει με τη σειρά της να επιδείξει πολύ αξιόλογες κατασκευές, όπως η γέφυρα Τατάρνας (Αιτωλοακαρνανίας) και Σερβίων (Κοζάνης).

Η άνθηση, όμως, της ελληνικής γεφυροποιίας έρχεται μετά το 1985, με πρωτεργάτη τη νέα, υψηλή γέφυρα Χαλκίδας. Πολλά και καλά έργα κατασκευάστηκαν έκτοτε με κοινοτικά κονδύλια στην ΠΑΘΕ, στην Εγνατία Οδό, αλλά μέσα στην Αθήνα. Το σημαντικότερο από τα σύγχρονα έργα είναι, δίχως αμφιβολία, η γέφυρα Ρίου-Αντιρρίου, όχι τόσο λόγω της κλίμακας, αλλά λόγω των δυσκολιών που κλήθηκε να υπερκεράσει. Ως αποτέλεσμα πλέον έχει αναπτυχθεί στη χώρα μας εξαιρετικά μεγάλη μελετητική και κατασκευαστική εμπειρία σχεδόν σε όλα τα είδη των γεφυρών. Μια εμπειρία χρήσιμη σήμερα για τις πιο εξωστρεφείς από τις ελληνικές κατασκευαστικές και μελετητικές εταιρίες.

Με αφορμή την πρόσφατη ολοκλήρωση της γέφυρας Τσακώνας, η οποία αναμένεται να δοθεί στην κυκλοφορία μέσα στον Ιανουάριο, η «Κ» παρουσιάζει τέσσερις από τις πιο σημαντικές σύγχρονες γέφυρες, η καθεμία με τα δικά της εξαιρετικά χαρακτηριστικά. Τη «γέφυρα των βραβείων» Ρίου-Αντιρρίου, την πρωτοπόρο υψηλή γέφυρα της Χαλκίδας, τις καινοτόμες γέφυρες Μετσόβου στην Εγνατία Οδό και Τσακώνας στην εθνική οδό Τρίπολης-Καλαμάτας.

ΡΙΟ - ΑΝΤΙΡΡΙΟ
Η 2η μεγαλύτερη καλωδιωτή στον κόσμο

Η γέφυρα-σταθμός έχει μήκος 2.883 μέτρων ξεκίνησε να κατασκευάζεται το 1997 και λειτούργησε στις 12 Αυγούστου 2004, έχοντας κοστίσει 630 εκατ. ευρώ.

Μέχρι πριν από δύο χρόνια ήταν η μεγαλύτερη καλωδιωτή γέφυρα πολλαπλών ανοιγμάτων στον κόσμο (σήμερα είναι η 2η). Για τη δημιουργία της χρησιμοποιήθηκαν καινοτόμες μελέτες και μέθοδοι κατασκευής. Η γέφυρα Ρίου-Αντιρρίου είναι ένα πραγματικό επίτευγμα της μηχανικής και έχει συγκεντρώσει πλήθος διεθνών διακρίσεων.

Το έργο έπρεπε να υπερκεράσει μια σειρά από ανυπέρβλητες μέχρι τότε δυσκολίες: Το πλάτος του στενού είναι 2,5 χιλιόμετρα και το βάθος του μεγάλο (65 μέτρα). Τα εδάφη στον πυθμένα του Κορινθιακού είναι χαλαρά, επομένως η συμβατική θεμελίωση ήταν αδύνατη. Επιπλέον, η περιοχή είναι εξαιρετικά σεισμογενής.

Η καλωδιωτή γέφυρα Ρίου-Αντιρρίου, μήκους 2.883 μέτρων, ξεκίνησε να κατασκευάζεται το 1997 και λειτούργησε στις 12 Αυγούστου 2004, έχοντας κοστίσει 630 εκατ. ευρώ. Κατασκευάστηκε από ιδιωτική κοινοπραξία με σύμβαση παραχώρησης (πρώτη φορά για γέφυρα στη χώρα μας), με βάση την οποία η εταιρεία Γέφυρα Α.Ε. θα συντηρεί, λειτουργεί και εκμεταλλεύεται το έργο έως 42 έτη.

Είναι δύσκολο να εξηγήσεις εν συντομία τον τρόπο που η γέφυρα κατασκευάστηκε. Για τη στήριξή της επελέγη η «αβαθής θεμελίωση», δηλαδή η βελτίωση των πρώτων 30 μέτρων του πυθμένα με μεταλλικά ενθέματα, στα οποία «ακουμπούν» τα θεμέλια, χωρίς να είναι συνδεδεμένα. Η κατασκευή αυτή επιτρέπει στη θεμελίωση να ανασηκωθεί ελαφρά ή να ολισθήσει κατά τη διάρκεια σεισμού.

Ένα άλλο σημαντικό χαρακτηριστικό της είναι το συνεχές καλωδιωτό κατάστρωμα, το οποίο είναι πλήρως αναρτημένο. Με τη βοήθεια αποσβεστήρων στους πυλώνες και στα ακρόβαθρα, η γέφυρα έχει αποκτήσει την απαραίτητη ευκαμψία σε περίπτωση σεισμού. Ταυτόχρονα το κατάστρωμα συνδέεται με τους πυλώνες με μια μεταλλική ράβδο, η οποία το σταθεροποιεί έναντι των ανέμων.

- Μελετητής: GTM (Vinci)- SEEE- ΔΟΜΗ Α.Ε.
- Κατασκευαστής: Κοινοπραξία Γέφυρα Α.Ε.

ΧΑΛΚΙΔΑ
Πρωτοποριακή για τη δεκαετία του ’80

Η κατασκευή της νέας γέφυρας ανάμεσα στη Στερεά Ελλάδα και στην Εύβοια ήταν ένα στοίχημα. Στα οκτώ χρόνια που διήρκεσε (1985-1993) χρειάστηκε να γίνουν εξειδικευμένες μελέτες και εργαστηριακές δοκιμές ώστε να καλυφθούν τα προβλήματα που παρουσιάζουν έργα αυτού του είδους. Η πρώτη καλωδιωτή γέφυρα της χώρας μας έχει συνολικό μήκος 694,5 μέτρα, πλάτος 14,10 μέτρα και οι πυλώνες της φθάνουν σε ύψος τα 90 μέτρα. Αποτελείται από τρία τμήματα: τις δύο προσβάσεις της από Εύβοια και Βοιωτία και το κεντρικό τμήμα μήκους 395 μέτρων, που είναι καλωδιωτό. Το καλωδιωτό τμήμα της γέφυρας έχει 3 ανοίγματα (90, 215 και 90 μέτρων αντίστοιχα) και 2 πυλώνες ύψους 90 μέτρων.

Κατά τη διάρκεια της κατασκευής, οι θερμοκρασίες που αναπτύσσονταν στην περιοχή έκαναν τους πυλώνες να «γέρνουν», λόγω διαστολής, προς τη σκιερή τους πλευρά. Όταν το πρόβλημα λύθηκε, με τη βοήθεια πολύ εξελιγμένων για την εποχή ηλεκτρονικών υπολογιστών, ξεκίνησε η κατασκευή του καταστρώματος, που «κρέμεται» σε 144 αναρτήρες, αποτελούμενους από πολλά επιμέρους συρματόσχοινα. Το κατάστρωμα κατασκευάστηκε με δύο προωθούμενες μεταλλικές πλατφόρμες. Ιδιαίτερη δυσκολία παρουσίασε το «φίλημα» (η ένωση) των δύο πλευρών του καταστρώματος, καθώς λόγω συστολής/διαστολής μετακινούνταν κατά 5 εκατοστά από το πρωί έως το απόγευμα. Χρειάστηκε να τοποθετηθεί ειδικός νάρθηκας, ώστε να σκυροδετηθεί το τελευταίο, μεσαίο κομμάτι (κλείδα).

Μοναδικό παγκοσμίως είναι το πάχος του οδοστρώματος, μόλις 45 εκατοστά, που δίνει στη γέφυρα αέρινη εμφάνιση. Η γέφυρα εγκαινιάστηκε στις 9 Ιουλίου 1993 και κόστισε συνολικά 3,25 δισ. δραχμές (9,5 εκατ. ευρώ). Σημειώνεται ότι επιθεωρήθηκε και συντηρήθηκε για πρώτη φορά το 2011-2012 και, όπως αποδείχθηκε, ήταν σε εξαιρετική κατάσταση, παρά τον κυκλοφοριακό φόρτο και τους σεισμούς.

• Μελετητής: ΔΟΜΗ Α.Ε.
• Κατασκευαστής: Ελληνική Τεχνοδομική ΑΕ-ΤΕΒ Α.Ε.

ΜΕΤΣΟΒΟ
150 μέτρα πάνω από το έδαφος

Η «προβολοδόμηση», δηλαδή η κατασκευή της γέφυρας συμμετρικά γύρω από τα βάθρα της (υπεραπλουστευμένα, η γέφυρα κατασκευάζεται εκατέρωθεν κάθε κολόνας, σαν «μπαλκόνι» που επεκτείνεται ώσπου να συναντήσει το διπλανό του), είναι ίσως η πιο δύσκολη και δαπανηρή μέθοδος κατασκευής. Είναι όμως απαραίτητη όταν πρέπει να γεφυρωθούν απότομες και βαθιές χαράδρες. Στην Εγνατία Οδό 43 γέφυρες είναι κατασκευασμένες με αυτήν τη μέθοδο, αλλά ανάμεσά τους ξεχωρίζει η γέφυρα του Μετσόβου, που «γεφυρώνει» το φαράγγι μεταξύ Μετσόβου και Ανηλίου.

Η ιδιαιτερότητά της έγκειται στην κλίμακα: Η γέφυρα, συνολικού μήκους 536 μέτρων, φθάνει στα 150 μέτρα πάνω από το έδαφος. Ως αποτέλεσμα, όλα έπρεπε να γίνουν σε πολύ μεγάλο ύψος. Επιπλέον, τη μελέτη και την κατασκευή της δυσχέραιναν και οι εξαιρετικά ισχυροί άνεμοι, που μπορεί να φθάσουν τα 100 χλμ/ώρα, λόγω της βαθιάς χαράδρας.

Τα προβλήματα ξεπεράστηκαν με τη βελτίωση των μεθόδων κατασκευής. Για παράδειγμα, χρησιμοποιήθηκαν οπλισμοί (μεταλλικοί ράβδοι μέσα στο σκυρόδεμα) μεγάλου μήκους, οι οποίοι αποκατέστησαν τη συνέχεια της γέφυρας σε μεγάλα μήκη (ανάμεσα στις κολόνες), το μεγαλύτερο των οποίων φθάνει τα 235 μέτρα, ένα από τα μεγαλύτερα «ανοίγματα» για αυτού του τύπου τις γέφυρες. Ειδικές συνθέσεις σκυροδεμάτων έκαναν δυνατή την άντληση για σκυροδέτηση σε μεγάλα ύψη και μήκη. Η επιτυχής επίβλεψη και η ακριβής τοπογραφική παρακολούθηση της κατασκευής οδήγησε σχεδόν σε απόλυτα επιτυχή εφαρμογή των μελετών, ακόμη και όταν οι δυσκολίες ήταν πρωτοφανείς (για παράδειγμα, στην κατασκευή του μεγαλύτερου βάθρου, ύψους 110 μέτρων, προβλεπόταν απόκλιση από την κατακόρυφο έως 26 εκατοστά και στην πράξη ήταν μόλις 1-2 εκατ.). Η γέφυρα ξεκίνησε να κατασκευάζεται το 2005, παραδόθηκε στην κυκλοφορία στις 8 Απριλίου 2009 και κόστισε συνολικά περίπου 50 εκατ. ευρώ.

• Μελετητής: ΔΟΜΗ Α.Ε.
• Κατασκευαστής: ΑΚΤΩΡ

ΤΣΑΚΩΝΑ
Η... τοξωτή πρόκληση της Πελοποννήσου

Η νεότερη από τις γέφυρες είναι έτοιμη να παραδοθεί στην κυκλοφορία μέσα στον Ιανουάριο. Χρειάστηκε να περάσουν 9,5 χρόνια μέχρι να μελετηθεί και να κατασκευαστεί, για έναν βασικό λόγο: έπρεπε να γεφυρώσει μια εκτεταμένη περιοχή που κατολίσθησε το 2003, στηριζόμενη σε πολύ σαθρά εδάφη.

Η τοξωτή γέφυρα Τσακώνας έχει συνολικό μήκος 390 μέτρα και μέγιστο ελεύθερο άνοιγμα 300 μέτρα, το δεύτερο μεγαλύτερο στην Ελλάδα μετά τη γέφυρα Ρίου-Αντιρρίου.

Αποτελείται από δύο τμήματα: το πρώτο, μήκους 90 μέτρων (στην πλευρά της Τρίπολης), έχει σχεδιαστεί σαν «συμβατική» γέφυρα. Στο δεύτερο, μήκους 300 μέτρων, ο δρόμος αναρτάται από δύο τόξα από χάλυβα (ύψους 36 μέτρων), τα οποία με τη σειρά τους στηρίζονται σε δύο βάθρα (κολόνες). Η θεμελίωση του κεντρικού μεσοβάθρου της γέφυρας, που φέρει το μεγαλύτερο μέρος του βάρους της, είναι εντυπωσιακή, καθώς πραγματοποιείται με 4 φρέατα (πηγάδια) διαμέτρου 6 μέτρων, που φθάνουν σε βάθος 15 μέτρων και τα οποία καταλήγουν σε έναν γιγαντιαίο κεφαλόδεσμο διαστάσεων 31Χ23 μέτρων (σαν κεφάλι καρφιού).

Η κατασκευή και τοποθέτηση των τόξων της γέφυρας υπήρξε τεχνολογική πρόκληση, λόγω του μεγάλου πάχους και βάρους των χαλυβδοφύλλων. Τα τόξα αποφασίσθηκε να κατασκευασθούν στο εργοστάσιο σε δωδεκάμετρα κομμάτια. Κατόπιν μεταφέρθηκαν στο εργοτάξιο, ανυψώθηκαν με γρύλους και συρματόσχοινα (με τη μέθοδο heavy lifting) και «ακούμπησαν» προσωρινά πάνω σε 7 ζεύγη χαλύβδινων πύργων ύψους μέχρι και 60 μέτρων. Αφού προσαρμόσθηκαν στην ακριβή τους θέση, συγκολλήθηκαν μεταξύ τους ώστε να διαμορφώσουν το ενιαίο τόξο. Λόγω του μεγάλου ύψους, αναπτύχθηκαν ειδικές διαδικασίες συγκολλήσεων και ελέγχων. Ο συνολικός προϋπολογισμός κατασκευής της γέφυρας ανέρχεται σε 22,8 εκατ. ευρώ.

• Μελετητής: ΔΟΜΗ Α.Ε.- ΕΔΑΦΟΣ Α.Ε.- ΣΥΣΤΑΣ Α.Ε.
• Κατασκευαστής: ΤΕΡΝΑ Α.Ε.

(Γιώργος Λιάλιος / Η ΚΑΘΗΜΕΡΙΝΗ, 03.01.2016, http://www.kathimerini.gr/844374/article/epikairothta/ellada/tesseris-gefyres---shmeia-anaforas-gia-to-mellon)

Impressive Video Modes of a Suspension Bridge

https://www.youtube.com/watch?v=dxoB5dYZg_Y

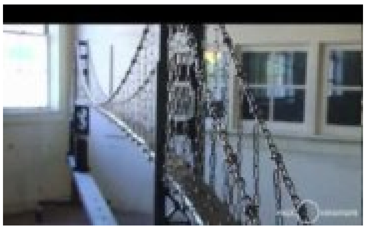

Golden Gate Bridge Dynamics / Science in the City / Exploratorium

Admit it: Hasn't the Godzilla inside you always wanted to grab the Golden Gate Bridge and shake it silly? Finally, you can. In honor of the iconic span's 75th birthday, Exploratorium exhibit developer Dave Fleming presents a dynamic model of the...

ΗΛΕΚΤΡΟΝΙΚΑ ΠΕΡΙΟΔΙΚΑ

www.geoengineer.org

Κυκλοφόρησε το Τεύχος #130 του **Newsletter του Geoengineer.org** (Ιανουαρίου 2016) με πολλές χρήσιμες πληροφορίες για όλα τα θέματα της γεωμηχανικής. Υπενθυμίζεται ότι το Newsletter εκδίδεται από τον συνάδελφο και μέλος της ΕΕΕΕΓΜ Δημήτρη Ζέκκο (secretariat@geoengineer.org).

☙ ❧

International Journal of Geoengineering Case Histories

Vol. 3, Issue 2

http://casehistories.geoengineer.org/volume/volume3/issue2/issue2.html

Bengt H. Fellenius "Discussion of: Ground Improvement Using Preloading with Prefabricated Vertical Drains", IJGCH 3.2.1, pp. 67-72.

Jehan Zeb, Tahir M. Hayat, Aziz Akbar, M. Azam "Mangla Dam Raising: Effectiveness of Seepage Reduction Measures for Sukian Dyke", IJGCH 3.2.2, pp. 73-84.

Ashok K. Chugh, D.V. Griffiths "Stability Analyses of the 1981 San Luis Dam Slide", IJGCH 3.2.3, pp. 85-112.

Rama Mohan Pokhrel, Takashi Kiyota, Reiko Kuwano, Gabriele Chiaro, Toshihiko Katagiri, Itsuro Arai "Preliminary Field Assessment of Sinkhole Damage in, Pokhara, Nepal", IJGCH 3.2.4, pp. 113-125.

:

ΕΚΤΕΛΕΣΤΙΚΗ ΕΠΙΤΡΟΠΗ ΕΕΕΕΓΜ (2015 – 2018)

ΕΕΕΕΓΜ

Τομέας Γεωτεχνικής
ΣΧΟΛΗ ΠΟΛΙΤΙΚΩΝ ΜΗΧΑΝΙΚΩΝ
ΕΘΝΙΚΟΥ ΜΕΤΣΟΒΙΟΥ ΠΟΛΥΤΕΧΝΕΙΟΥ
Πολυτεχνειούπολη Ζωγράφου
15780 ΖΩΓΡΑΦΟΥ

Τηλ. 210.7723434
Τοτ. 210.7723428
Ηλ-Δι. secretariat@hssmge.gr ,
geotech@central.ntua.gr
Ιστοσελίδα www.hssmge.org (υπό κατασκευή)

«ΤΑ ΝΕΑ ΤΗΣ ΕΕΕΕΓΜ» Εκδότης: Χρήστος Τσατσανίφος, τηλ. 210.6929484, τοτ. 210.6928137, ηλ-δι. ctsatsanifos@pangaea.gr, editor@hssmge.gr, info@pangaea.gr

«ΤΑ ΝΕΑ ΤΗΣ ΕΕΕΕΓΜ» «αναρτώνται» και στην ιστοσελίδα www.hssmge.gr